Mistaking plastic for zooplankton: risk assessment of plastic ingestion in the Mediterranean sea

[Fabri-Ruiz, S[1,2]., Baudena, A[1]]*., Moullec F[3]., Lombard, F.[1], Irisson, J.-O[1]., Pedrotti, M.L[1].

[1]Sorbonne Université, CNRS, Laboratoire d'Océanographie de Villefranche, Villefranche-sur-Mer, France

[2] DECOD (Ecosystem Dynamics and Sustainability), IFREMER, INRAE, Institut Agro, Nantes, France

[3]Department of Coastal Systems, Royal Netherlands Institute for Sea Research, P.O. Box 59, 1790 AB Den Burg, Texel, The Netherlands

Corresponding authors: alberto.baudena@gmail.com, salome.fabri.ruiz@ifremer.fr

*co-first authors

Abstract

Floating plastic debris is a pervasive pollutant in seas and oceans, affecting a wide range of animals. In particular, microplastics (< 5 mm in size) increase the possibility that marine species consume plastic and enter the food chain. The present study investigates this potential mistake between plastic debris and zooplankton by calculating the plastic debris to zooplankton ratio over the whole Mediterranean Sea. To this aim, in situ data from the Tara Mediterranean Expedition are combined with environmental and Lagrangian diagnostics in a machine learning approach to produce spatially-explicit maps of plastic debris and

zooplankton abundance. We then analyse the plastic to zooplankton ratio in regions with high abundances of pelagic fish. Two of the major hotspots of pelagic fish, located in the Gulf of Gabès and Cilician basin, were associated with high ratio values. Finally, we compare the plastic to zooplankton ratio values in the Pelagos Sanctuary, an important hotspot for marine mammals, with other Geographical Sub-Areas, and find that they were among the larger of the Western Mediterranean Sea. Our results indicate a high potential risk of contamination of marine fauna by plastic and advocate for novel integrated modelling approaches which account for potential trophic transfer within the food chain.

I. Introduction

Plastic pollution is ubiquitous in the global ocean, from the sea surface to the seafloor (Woodall et al. 2014, Esposito et al., 2022), and represents a major threat to socio-economic services, tourism, and, ultimately, marine ecosystems (Aretoulaki et al., 2021; Beaumont et al., 2019). It is estimated that 19 to 23 million metric tons of plastic waste entered the aquatic systems in 2016, with an increasing trend expected in the next few years (Borrelle et al., 2020; Lau et al., 2020). The Mediterranean Sea is among the world's seas most polluted by plastic (Gerigny et al., 2019), with levels of concentration similar to those found in the Great Pacific Garbage Patch (Cózar et al., 2015; Pedrotti et al., 2022). At the same time, this quasi-enclosed sea is a key hotspot of marine biodiversity, with more than 17 000 species recorded (Coll et al., 2010), and supports an overall fishery activity of ca. 9 billion dollars every year (FAO 2020). Mediterranean marine ecosystems are, therefore, highly sensitive to plastic pollution (Solomando et al., 2022; Soto-Navarro et al., 2021). Understanding the magnitude of the impact of this pollutant on marine life is essential for conservation and mitigation strategies

(Galgani et al., 2014; Kershaw et al., 2019). In particular, it is fundamental to evaluate the risk of plastic transfer along marine trophic webs, including humans as well (Provencher et al., 2019; Rochman et al., 2015; Savoca et al., 2021). The need to assess microplastic risk at the scale of the Mediterranean sea is important considering the long distances crossed by mobile organisms (ie. cetaceans, fish, …). With the increase of multiple anthropogenic pressures (including microplastics) on these species, the risks must be evaluated at an appropriate spatial scale to mitigate their effect with adapted conservation measures. However, this understanding is hampered by the scarcity of available data, which usually cover only limited portions of the basin and differ in methodology (e.g., Mansui et al., 2020). In addition, only few studies measured plastic and organism concentrations concomitantly (Gérigny et al., 2022), making understanding of plastic impact difficult. In addition, the role of circulation on the distribution of plastic and zooplankton organisms is poorly unknown to date. An alternative method to estimate plastic concentration is the use of Lagrangian models. These are based on the release of virtual plastic particles which are then advected by current fields. From the virtual plastic trajectories different information can be obtained, including zones of potential accumulation or passage of plastic debris (Baudena et al., 2022, 2019; Beaumont et al., 2019; Liubartseva et al., 2019; Mansui et al., 2020) dispersion. Only a few have, however, been validated quantitatively with in situ data to date (Baudena et al., 2022). Furthermore, Lagrangian models only simulate plastic dispersion, and usually do not include biological activity such as the presence of zooplankton.

In the present study, we aim to quantify the relative presence of plastic compared to that of zooplankton, to assess the potential mistake encountered by marine predators. For this purpose, we used in situ observations from the Tara Mediterranean Expedition, which

67 constitutes the largest plastic dataset in the Mediterranean Sea to date: 122 stations covering
68 the entire basin with homogenised and standardised sampling techniques. We considered
69 plastic debris between 0.33—5.00 mm (usually referred to as *microplastics*[1][2]).
70 Microplastics constituted an important proportion of the plastic debris at sea, and were the
71 vast bulk (~95%) of the debris collected during the Tara Mediterranean Expedition, making
72 plastic estimates more reliable (Pedrotti et al., 2022). Importantly, along with plastic debris,
73 zooplankton organisms of the same size class (0.33—5.00 mm) were concomitantly sampled.
74 We then combined them with a machine learning approach to study the environmental
75 drivers of plastic and zooplankton concentrations, unravelling some physical processes
76 responsible for their distribution. With this information, we obtained spatial predictions for
77 the whole Mediterranean Sea surface layer. These quantities were used to estimate a ratio
78 between plastic debris and zooplankton abundance. This value represents the proportion of
79 plastic debris with respect to the zooplankton organisms and can be seen as an indicator of
80 potential impact on marine life. A ratio of 0.1 means that, for every ten zooplankton
81 organisms present in a given seawater parcel, one plastic debris is present as well. Previous
82 studies only estimated this metric in correspondence with the location of the sampling
83 stations (Cole et al., 2011; Collignon et al., 2014; Doyle et al., 2011; Gérigny et al., 2022; Gove
84 et al., 2019 (plastic:larval Fish) ; Lattin et al., 2004; Moore et al., 2002; Pedrotti et al., 2016).
85 However, for conservation purposes, information on the impact of plastic at larger spatial
86 scales is needed: here, we provide an estimate over the entire Mediterranean Sea of both
87 plastic and zooplankton abundances as well as their ratio.

88 Furthermore, we use this metric to assess the overlap with potential predators through two
89 illustrative case studies. In the first, we only consider (i) species for which plastic ingestion has

been reported (Fossi et al., 2014; Lefebvre et al., 2019; Pennino et al., 2020); (ii) species which are known to adopt non selective feeding strategies for certain prey sizes (Garrido et al., 2008, 2007; Queiros et al., 2019), as they could not be able to distinguish between plastic debris and zooplankton; (iii) species which are widely distributed over the entire Mediterranean basin (Bray et al., 2019); (iv) plastic debris and zooplankton in the same size class (0.33—5.00 mm) which can potentially confuse predators. As potential predators, we consider small pelagic fish (such as anchovies or sardines), which can acquire food through filter feeding behaviour. They feed on organisms smaller than 5 mm in size (Le Bourg et al., 2015) and have an important ecological and socio-economic role in the Mediterranean Sea. In the second case study, we focus on cetaceans by investigating the ratio values in the Pelagos sanctuary, which is a key foraging ground for marine mammals in the northwestern Mediterranean Sea (Croll et al., 2018; Fossi et al., 2014), and comparing them with Geographical Sub-Areas (GSAs) in the Mediterranean.

II. Materials and Methods

We used a machine learning approach to correlate the response (i.e., in situ plastic and zooplankton abundances data obtained from the Tara Mediterranean Expedition) and explanatory (i.e., physical and biogeochemical data and Lagrangian and Eulerian diagnostics) variables. In the following sections, we described the data and the modelling framework used as well as the methodology employed to determine the plastic to zooplankton ratio, which is then applied to two case studies. To ensure reproducibility and transparency of results, we provided an ODMAP (Overview, Data, Model, Assessment and Prediction) protocol in the Supplementary Material. ODMAP is a standard protocol for species distribution models

based-approach that we used in our study (Fitzpatrick et al., 2021; Zurell et al., 2020).

2.1. Response variables: in situ plastic and zooplankton data from Tara Mediterranean Expedition

The Tara Mediterranean Expedition was conducted in the Mediterranean Sea between June and November 2014. It sampled plastic debris and zooplankton in 122 stations across the whole basin (Figure 1), representing the largest coupled plastic zooplankton database in the Mediterranean Sea to date (Pedrotti et al., 2022). Plastic items were collected with a manta net (height 25 cm, width 60 cm, mesh size 333 µm) towed at the sea surface and at an average speed of ~2.5 knots for 60 minutes over a mean distance of ~4 km. Details of plastic processing are described in Pedrotti et al., (2022), and are briefly reported here. Plastic items were manually separated from zooplankton and organic tissue and scanned using the ZooScan system (Gorsky et al., 2010) under dry conditions, while zooplankton organisms were scanned separately under aqueous conditions. Particles and zooplankton were automatically detected and their morphological attributes were extracted by post-processing with Zooprocess and Plankton Identifier software. All obtained images were imported within EcoTaxa (http://ecotaxa.obs-vlfr.fr, Picheral et al., 2017) and classified in different taxonomic or particle categories. Microplastic (0.33—5 mm) abundances (in items per square km; N/km^2) were calculated from particle counts. In addition, plastic debris abundance was calculated also for the following size classes: debris between 0.33—1 mm; debris between 1—5 mm; all plastic debris collected (i.e., larger than 0.33 mm). The size class limits were chosen in order to test the robustness of the results. Similarly, total zooplankton abundance per sample was calculated from zooscan and under the same size classes defined for plastic debris abundance.

Diel vertical migration was not observed over the 24 hour day (Figure S1)

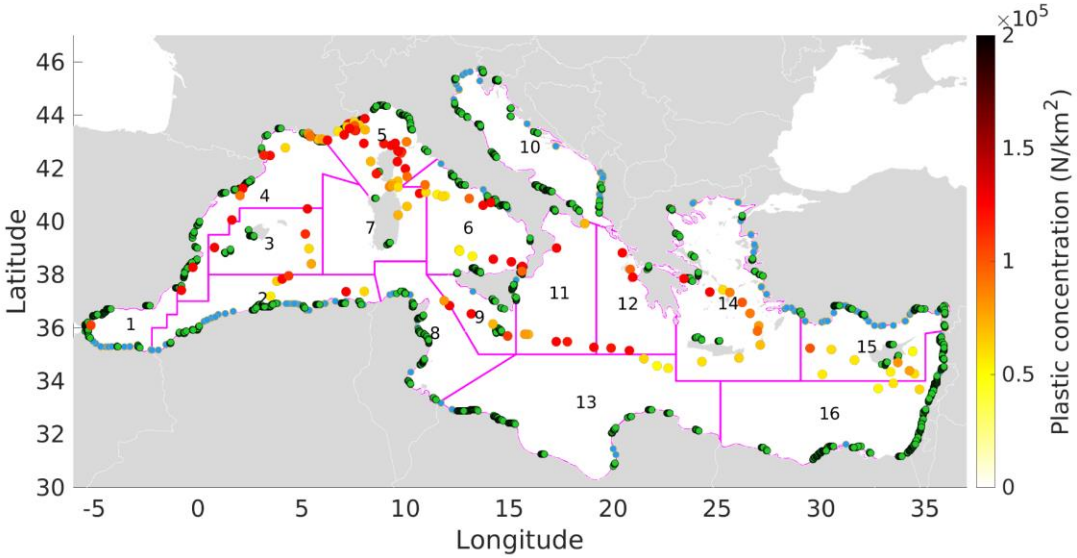

Figure 1 : Overview of the domain studied: Location of the 122 Tara Mediterranean Expedition stations (colored circles) and corresponding estimated plastic concentrations (right-hand yellow-to-red scale bar). Green and blue dots indicate the position of the coastal cities and river mouths used as potential plastic sources. The purple dashed lines separate the different Geographical Sub-Areas (GSAs) investigated in this study, indicated by a number. 1: Alboran Sea, 2: Algeria, 3: Balearic Islands, 4: Northern Spain and Gulf of Lion, 5: Pelagos sanctuary, 6: Tyrrhenian Sea, 7: Sardinia, 8: Tunisia, 9: Southern Sicily and Malta, 10: Adriatic Sea, 11: Western Ionian Sea, 12: Eastern Ionian Sea, 13: Southern Ionian Sea, 14: Aegean Sea, 15: Northern Levant Sea and Cyprus, 16 : Southern and Eastern Levant Sea

2.2. Explanatory variables

2.2.1. Physical and biogeochemical data : salinity, temperature, nitrates, phosphates, dissolved oxygen concentration

151 Physical and biogeochemical data were extracted from the Copernicus Marine Environment
152 Monitoring Service (CMEMS, http://marine.copernicus.eu, product
153 MEDSEA_REANALYSIS_PHYS_006_004) at 1/16° resolution. The product was supplied by the
154 Nucleus for European Modelling of the Ocean (NEMO), with a variational data assimilation
155 scheme (OceanVAR) for temperature and salinity vertical profiles and satellite Sea Level
156 Anomaly along track data. We only considered the surface layer (Simoncelli et al., 2014).
157 Physical and biogeochemical data were provided at daily and weekly resolution, respectively.
158 Climatologies were calculated by averaging over the six months of the Tara Mediterranean
159 Expedition (June to November 2014; Table S1). Spatial resolution was decreased from 1/16°
160 to 1/8° by bilinear interpolation to fit the same spatial resolution of the Lagrangian and
161 Eulerian diagnostics. The environmental explanatory variables obtained include mean values
162 for temperature, salinity, phosphate, nitrate and dissolved oxygen concentration.
163 Zooplankton concentration (mass content of zooplankton expressed as carbon in seawater,
164 g/km^2; Seapodym model; Lehodey et al., 2010) provided by the
165 GLOBAL_MULTIYEAR_BGC_001_033 product (CMEMS platform) was used to calculate a
166 zooplankton climatology between June and November 2014 at 0.083° spatial resolution. The
167 latter was used as a qualitative reference for the zooplankton projection (Subsec. 4.1), and
168 not as an explanatory variable.

169 **2.2.2. Lagrangian and Eulerian diagnostics**

170 **Velocity field and trajectory calculation:** The velocity field was obtained by combining
171 together two hydrodynamical fields, both downloaded from the CMEMS platform. The first
172 product was the MEDSEA_REANALYSIS_PHYS_006_004, which provides surface currents and
173 includes the geostrophic and the Ekman components. It has a spatial resolution of 1/16° and

a temporal resolution of one day. The second product was the MEDSEA_HINDCAST_WAV_006_012. It provides drift due to waves (Stokes drift). It has a spatial resolution of 1/24° and a temporal resolution of one day. The velocity fields were spatially and temporally interpolated (bilinear interpolation) and summed together, providing the final velocity field (1/24°; 1 hour). Thus, the surface currents used take into account the Stokes drift, which indirectly includes windage, an important component for microplastic transport in marine environments (Onink et al., 2019), especially in the Mediterranean Sea (Liubartseva et al., 2018). As zooplankton samplings were collected at the same depth as plastic debris, we used the same velocity field for both explanatory variables. Trajectories were calculated with a 4^{th} order Runge-Kutta scheme in both space and time, with a time step of 20 minutes.

Lagrangian and Eulerian diagnostics description: Different Lagrangian and Eulerian diagnostics were used as explanatory variables. Lagrangian diagnostics were derived from trajectories, whereas Eulerian diagnostics were obtained by properties at a fixed location. The Eulerian diagnostics calculated were: *Absolute velocity*: $U=\sqrt{u^2+v^2}$, with *u* and *v* being the zonal and meridional component of the velocity field; *Kinetic Energy* = u^2+v^2 which, together with the absolute velocity is considered as a proxy of the intensity of the currents; *Vorticity*: denotes the presence (when positive or negative) or absence (when close to 0) of eddies; *Okubo-Weiss*: When negative (positive), this metric indicates a water parcel inside (outside) an eddy; *Turbulent Kinetic Energy (TKE)*: This metric analyses the standard deviation of the velocity field time series and quantifies whether a region was subjected to strong turbulence. The Lagrangian diagnostics calculated were: *Finite-Time Lyapunov Exponents (FTLE)*: FTLEs quantify the rate of separation due to currents. They are used to identify barriers to transport

or regions affected by strong turbulence (Baudena et al., 2021; d'Ovidio et al., 2004); *Lagrangian Betweenness*: this metric is used to identify regions that act as "bottlenecks" for the circulation, i.e. in which water parcels of multiple origins pass and then go to several different destinations (Ser-Giacomi et al., 2021); *Retention time*: this metric estimates the amount of time a water parcel spent inside an eddy (if it was inside it) (d'Ovidio et al., 2015); *Lagrangian divergence*: this metric calculates the Eulerian divergence along the backward trajectory. When negative (positive), it indicates convergence (divergence) of water masses, and can be used as a proxy of downwelling (upwelling) Hernández-Carrasco et al., (2018); *Lagrangian Plastic Pollution Index (LPPI)*: this metric estimates the amount of plastic debris in a water parcel based on the plastic sources (cities and rivers, blue and green dots in Fig. 1) encountered along the water parcel's previous path. The water parcel "encounters" a plastic source when it passes below a distance threshold from it (details in Pedrotti et al., 2022).

As for the physical and biogeochemical explanatory variables, climatologies of Lagrangian and Eulerian diagnostics were calculated between June and November 2014 at 1/8° of spatial resolution over the entire Mediterranean Sea. Details about the different parameters used for each of the diagnostics are reported in Supplementary Table S2.

2.3. Modelling framework: Xgboost models

2.3.1. Collinearity between explanatory variables

Multicollinearity occurs when two or more explanatory variables in a multiple regression model are highly correlated, which means that one can be predicted linearly from the others with a high degree of accuracy. Multicollinearity can cause data redundancy in the explanatory variables which can lead to model overfitting or reduction in model predictive ability (Dormann et al., 2013). If multicollinearity patterns differ between fitted data in the

model and new data, large errors could be introduced in the predictions. To restrict these possible biases, multicollinearity between explanatory variables was initially examined using variance inflation (VIF) factors in a stepwise procedure (Dormann et al., 2013). VIF is computed from equation [1], where R^2_j is obtained from a regression between variable j^{th} against all other explanatory variables.

$$VIF_j = \frac{1}{1-R_j^2} \quad [1]$$

In a stepwise procedure, the function calculates VIF values for all explanatory variables, removes the variable with the highest value, and repeats until all VIF variable values are below a given threshold (here 5). Finally, we computed Spearman pairwise correlation (r_S) between descriptors and removed one of the two descriptors when correlation values of r_S were above 0.7 (Dormann et al., 2013). Analyses were performed using the usdm (Babak, 2015) and corrplot (Wei et al., 2017) R packages. Table S3 lists the remaining variables used in Xgboost models for each category.

2.3.2. Parameterization and calibration of XGboost models

The extreme gradient boosting (XGBoost) modelling approach (Chen and Guestrin, 2016) was used to model plastic debris and zooplankton abundances for each size class. Xgboost is an efficient gradient machine learning method that combines two algorithms: first, simple and small regression trees, calculated on random subsets of data while minimising residuals; and subsequently boosting, which combines all the models into a unique solution (for statistical details see Chen and Guestrin, 2016). XGBoost models are able to fit complex functions, which could reflect the complexity of processes shaping plastic debris and zooplankton patterns.

Xgboost models were performed using the xgboost R package (Chen et al., 2015). Cross validation procedure was used to estimate the best parameters of the xgboost model. This procedure uses a single parameter k that refers to the number of groups for a given dataset to be split into. In our case, we used k=4. For each group, we take the remaining groups as a training data set and use the selected group to evaluate the model. This procedure was performed for different xgboost parameters and poisson distribution: number of trees (1 to 900), maximum depth (2, 4, 6) where the higher is the value the more complex the model is, eta (0.005, 0.01, 0.02, 0.03, 0.04) which is the learning rate, min_child_weigth (1, 5) which defines the minimum sum of weights of all observations required in a child (used to control over-fitting). Best parameters were selected by minimising the negative log-likelihood for Poisson regression. We evaluated the model using the R^2 coefficient between observed and predicted data. Because several distance threshold values were provided for plastic data (based on the LPPI), we fitted models for each and kept the best one (Table S4).

2.3.3. Prediction and projection

The partial dependence plots (PDP) technique (Friedman, 2001) was used to achieve a graphical representation of the marginal effect of a variable on the response variable. We also extract variable importance from the model, which shows how a feature is important in making a branch of a decision tree purer. A high percentage means important explanatory variables which constrain response variables. Calculated functions in the model were then used to extrapolate plastic debris and zooplankton abundances for each grid cell over the entire Mediterranean Sea at a period corresponding to June-November 2014. We projected mean plastic debris and zooplankton abundances and associated standard deviations.

2.4. Plastic to zooplankton ratio definition

Using zooplankton and plastic debris abundance projections over the entire Mediterranean Sea, we calculated the plastic debris to zooplankton ratio (amount of plastic debris divided by the amount of zooplankton) at 1/8° of spatial resolution. For each grid cell *i*, the ratio was obtained by dividing the plastic and the zooplankton abundances (expressed in N/km^2) of the same size class *j*:

$$Ratio_{i,j} = \frac{Plastic\ abundance_{i,j}}{Zooplankton\ abundance_{i,j}} \quad (1)$$

Equation 1 implies that, for example, if the ratio equals 0.1, for every 1000 zooplankton organisms in a given water parcel 100 plastic debris of similar size is present. The ratio was calculated using plastic debris and zooplankton organisms of size classes between 0.33—5 mm. Ratios calculated using different size classes (Subsec. 2.1) are reported in Supplementary Materials. The uncertainty on the ratio was calculated with the variance formula using the plastic and zooplankton associated standard deviations and Equation (1).

The ratio obtained using the size class of 0.33—5 mm was evaluated (i) in the Pelagos Sanctuary, a hotspot for cetaceans, representing a foraging ground for different whale species (Morgado et al., 2017). The ratio in the Pelagos Sanctuary was compared with the ratio calculated in the Mediterranean GSAs (Fig. 1). GSAs were obtained from the FAO platform (https://www.fao.org/gfcm/data/maps/gsas/en/). In order to have GSAs of similar surface area, we merged together the following GSAs: Northern Alboran Sea, Southern Alboran Sea, and Alboran Island, creating the Alboran Sea GSA (GSA 1); Northern Spain and Gulf of Lion GSA (GSA 4); Ligurian Sea and Northern Tyrrhenian Sea and Southern and Central Tyrrhenian Sea, creating the Tyrrhenian Sea GSA (GSA 6); Western and Eastern Sardinia, creating the

290 Sardinia GSA (GSA 7); Northern Tunisia, Gulf of Hammamet, and Gulf of Gabès, creating the
291 Tunisia GSA (GSA 8); Southern Sicily and Malta GSA (GSA 9); Northern and Southern Adriatic
292 Sea, creating the Adriatic Sea GSA (GSA 10); Crete and Aegean Sea, creating the Aegean Sea
293 GSA (GSA 14); Northern Levant Sea and Cyprus, creating the Northern Levant Sea and Cyprus
294 GSA (GSA 15); Southern and Eastern Levant Sea GSA (GSA 16). In addition, the Corsica GSA
295 was not considered because it was included in the Pelagos Sanctuary, while the Gulf of Lion
296 and Ligurian Sea and Northern Tyrrhenian Sea were reduced to avoid overlap with the Pelagos
297 Sanctuary.
298 The ratio values in the Pelagos Sanctuary and in the GSAs were compared using a paired
299 sample Wilcoxon test with corrections applied for multiple testing; (ii) in the Mediterranean
300 areas where the total biomass of small pelagic fish is large according to simulations provided
301 by the end-to-end ecosystem model OSMOSE-MED (Moullec et al., 2019b). Results for the
302 other size classes are available in the Supplementary Material.
303
304 **2.5. The end-to-end model OSMOSE-MED**
305
306 OSMOSE-MED is an end-to-end modelling chain, including a general circulation model, a
307 regional climate model, a regional biogeochemistry model and a multispecies dynamic model
308 (OSMOSE; Moullec et al., 2019). OSMOSE is a spatially explicit individual-based model which
309 simulates the whole life cycle of several interacting fish and macro-invertebrates species from
310 eggs to adult stages. Major ecological processes of the life cycle, such as growth, predation,
311 reproduction, and mortality sources, are modelled step by step (15 days in this study)
312 (www.osmose-model.org; (Shin et al., 2004; Shin and Cury, 2001). OSMOSE-MED covers the
313 whole Mediterranean Sea and represents the Mediterranean food web from pankton to main

top-predators in the 2006-2013 period. Hundred marine species (fish, cephalopods and crustaceans), representing ca. 95% of total declared catches in the region over the 2006-2013 period were explicitly modelled. For a full description of the parameterization and calibration of OSMOSE-MED (see Moullec et al., 2022, 2019a, 2019b).

The biomass of small pelagic fish is an output of OSMOSE-MED simulations. As OSMOSE is a stochastic model, ten replicated simulations were run and averaged to analyse the outputs. For this study, the total biomass of 10 small pelagic species only (e.g., European anchovy, European sardine, Round sardinella or European sprat) was considered. Areas of small-pelagic high biomass were defined as the locations with a biomass value higher than the 90^{th} percentile of all the Mediterranean Sea biomass values. Results corresponding to the 80^{th} and 95^{th} percentiles are reported in the Supplementary Materials.

III. Results

3.1. Plastic and zooplankton distributions in the Mediterranean Sea and their drivers

The predictive performance of the Xgboost model was assessed by calculating the correlation coefficient (R^2) between observed and predicted values of plastic and zooplankton abundance (Table 1, S4, S5, Figure S2, S3). R^2 coefficients were 0.68 and 0.57 for plastic debris and zooplankton abundances, respectively (Table 1). Overall, the relationships found tended to overestimate low values and to underestimate large ones (Figure S2, S3). R^2 is known to be sensitive to the extent of dependent variables (Gelman and Hill, 2006) which range between 2260 N/km² and 7974561 N/km² in this study. This could explain the low cross-validated R^2 which is strengthened by the low amount of available data (122 sampling stations). High zooplankton abundances were associated with negative Okubo-Weiss values (19 % of the

337 explanatory power in the model, Fig. 2c), and with positive and negative vorticity values
338 (14%). Both these explanatory variables indicate an eddy presence, and do not reveal a clear
339 preference for cyclones or anticyclones. The temperature influenced the total zooplankton
340 abundance as well (16%), with lower abundances associated with higher temperatures.
341 Attracting fronts, identified by Finite-Time Lyapunov Exponents (FTLEs, 9%) calculated
342 backward in time, were positively correlated with zooplankton abundance, while the
343 relationship was of opposite sign with diverging fronts (FTLE forward in time: 8%; and
344 divergence: 7%). Explanatory variables that most contributed to explain plastic debris
345 abundance were the kinetic energy (50%) and TKE (10%) (Figure 2d), indicating a greater
346 concentration of plastic debris in retentive and low turbulence regions. Nitrates (11%, a proxy
347 for riverine outputs) indicated a positive relationship between plastic debris presence and the
348 proximity to river mouths.

349 When considering the plastic and zooplankton abundances projected over the entire
350 Mediterranean Sea (Fig. 2a,b), highest concentrations were mainly observed in the Adriatic
351 and Aegean Seas (GSAs 10 and 14 in Fig. 1, respectively). In these regions, abundances were
352 estimated around $20x10^6$ N/km^2 for zooplankton (Figure 2a) and $5x10^6$ N/km^2 for plastic
353 debris (Figure 2b). The Eastern basin (GSAs 15 and 16) presented low abundances of
354 zooplankton and plastic debris. However, the latter was abundant along Cyprus (located in
355 GSA 15) and Lebanon (located in GSA 16) coasts and in the Gulf of Gabès (located in GSA 8).
356 The Tyrrhenian Sea (GSA 6) was also a hotspot of plastic debris abundance. In the Strait of
357 Gibraltar (located in GSA 1), the models predicted high values of zooplankton abundances and
358 low plastic debris concentrations.

359 The results obtained with different size classes showed very similar patterns (Figure S4, S5

and S6), and high R^2 coefficients were obtained as well (Table S5). Plastic standard deviation maps (Fig. S7a) show that the uncertainties corresponded to about 10% of the plastic abundance values. The same considerations were valid for the zooplankton uncertainties (Fig. S7b), showing the robustness of the models obtained.

Table 1 : Predictive performance and best parameters estimated by 4-fold cross validation for size between 0.33 and 5 mm

	Predictive performance	**Model parameters**			
Group	**R^2**	**trees**	**Maximum depth**	**Eta**	**Minimum child weight**
Zooplankton (> 0.33 and < 5 mm)	0.57	707	2	0.04	5
Microplastic (> 0.33 and < 5 mm)	0.68	851	2	0.03	1

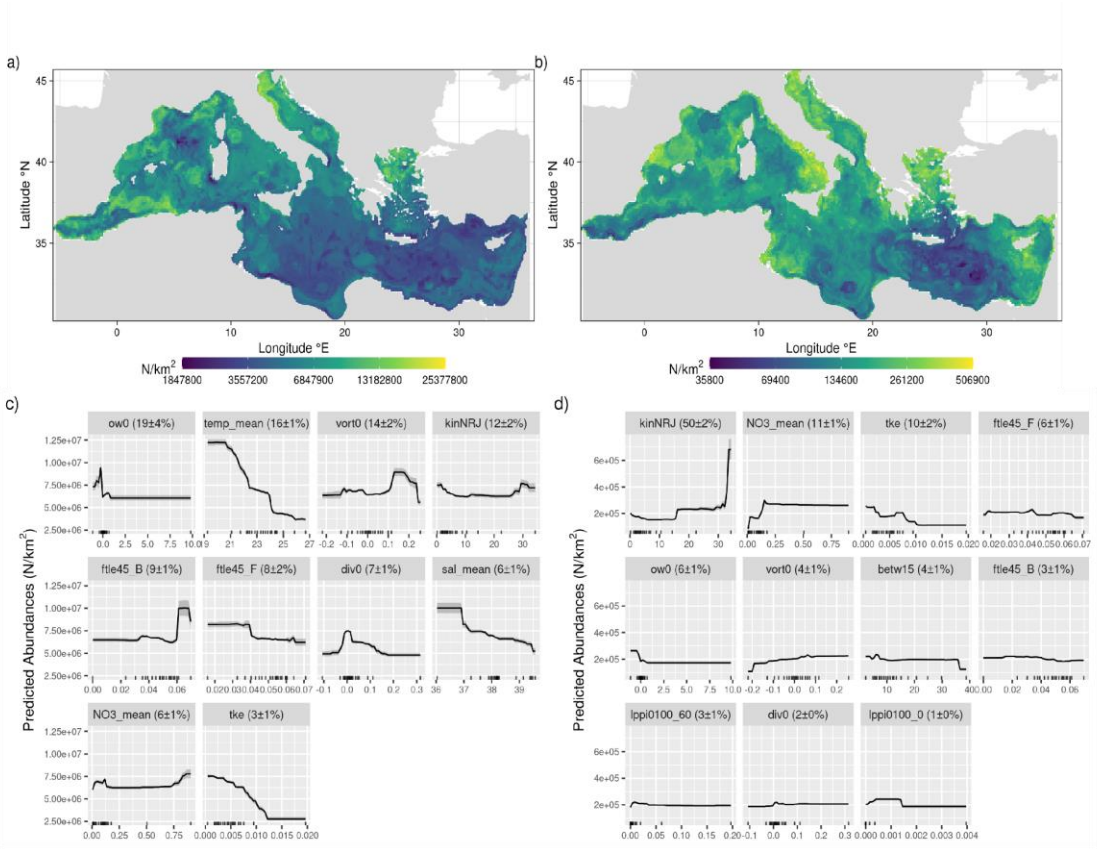

368

369 **<u>Figure 2</u> : Plastic and zooplankton abundances :** Spatial projection and partial dependence
370 plot of zooplankton (panels a and c, respectively) and plastic debris abundance (panels b and
371 d, respectively) for the size class < 5 mm. oW0 = Okubo Weiss, kinNRJ = Kinetic Energy,
372 temp_mean = mean temperature, NO3_mean = mean nitrate concentration, vort0 =
373 vorticity , tke = Turbulent Kinetic Energy, ftle45_F = FTLE 45 days forward in time, ftle45_B =
374 FTLE 45 days backward in time, div0 = Eulerian Divergence, betw15 = Betweenness at 15 days,
375 sal_mean = mean salinity, lppi0100_60 = LPPI with distance threshold of 1° and 60 days
376 backward in time, lppi0100_0 = LPPI with distance threshold of 1° and no advection

377 **3.2. Plastic to zooplankton ratio**

378 Using zooplankton and plastic debris abundance projections, we calculated the plastic to
379 zooplankton ratio (number of plastic debris per km^2 divided by the number of zooplankton

380 organisms per km^2 , MM 2.4) over the entire Mediterranean Sea for the size class between
381 0.33—5 mm (Fig. 3a). The average plastic to zooplankton ratio was 0.029 (±0.012) at the
382 Mediterranean scale. Areas with the highest average plastic to zooplankton ratio were the
383 gulf of Gabès (located in GSA 8), the Cilician (GSA 15), the Levantine (GSA 15 and 16), and the
384 Southern Tyrrhenian Seas (GSA 6), with values of ~0.10. Intermediate values (~0.05) were
385 found in the Balearic (GSA 3) and Adriatic Seas (GSA 3) and in the Central Mediterranean (GSA
386 13). Lower values (~ 0.01) were in the Alboran Sea (GSA 1) and the central sector of the
387 Eastern Mediterranean Sea (GSA 16 and eastern part of GSA 15).[3][4][5]

388 When considering the results obtained with different size classes the spatial pattern did not
389 change consistently (Fig. S10). The ratio decreased to 0.004—0.1 when considering a size class
390 between 0.33—1 mm, while it increased to 0.005—0.3 when considering the size class
391 between 1 and 5 mm, due to the different abundances considered. The uncertainty on the
392 ratio (Fig. S7c) was greater in regions of larger ratio and lower elsewhere, and corresponded
393 to ~10% of the ratio value. These results show the soundness of this metric.

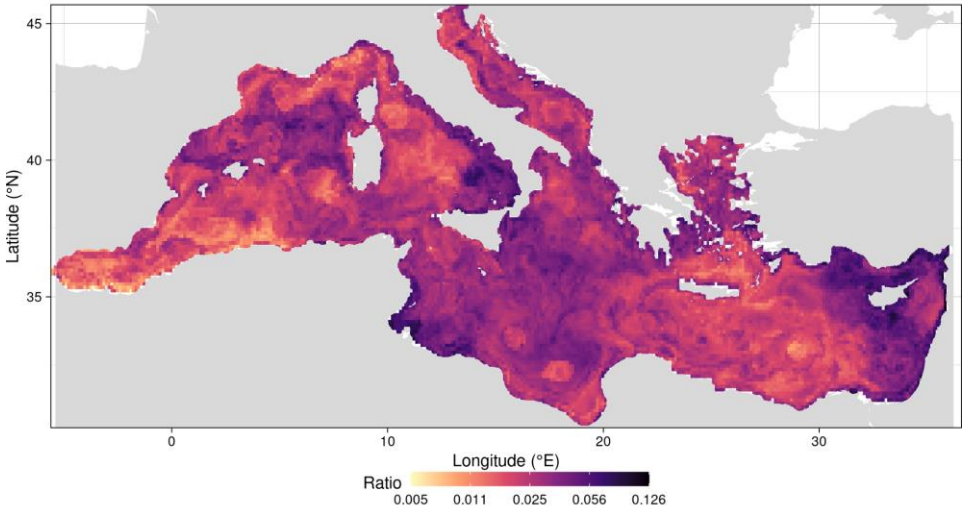

394

395 **Figure 3 : Plastic to zooplankton ratio** : Spatial projection of the plastic to zooplankton ratio

396 for the size class between 0.33—5 mm

397 **3.3. Case studies**

398

399 **3.3.1. Wildlife exposure: plastic ingestion risk for small pelagic fish**[6]

400

401 The plastic to zooplankton ratio was applied to two case studies to analyse the probability of

402 plastic ingestion by wildlife as described in the next subsections.

403 In the first case study, we considered the total biomass of small pelagic fish in the

404 Mediterranean Sea for the time period 2006-2013, obtained from the Osmose model.

405 One of the largest Mediterranean hotspots of small pelagic fish, located in the Gulf of Gabès

406 (located in GSA 8), as well as a smaller one in the Cilician basin (between Cyprus and Turkey,

407 GSA 15), were found in correspondence with plastic to zooplankton ratios greater than 0.06

(Fig. 4a). Two large hotspots of small pelagic fish, in the Adriatic Sea (GSA 10) and in the Southern Catalan Sea (GSA 4), were associated with moderate plastic to zooplankton ratios greater than 0.03. The remaining part of the small pelagic hotspots was highly patchy and mainly distributed along the coasts, with variable ratio values.

When using different percentiles to identify the main small pelagic fish hotspots (Fig. S9), these were still located in the Adriatic Sea and in the Gulf of Gabès, confirming that these hotspots were threatened by plastic pollution and providing evidence of the robustness of the analyses.

3.3.2 Wildlife exposure: plastic ingestion risk in the Pelagos Sanctuary and different Mediterranean regions

In the second case study, we calculated the plastic to zooplankton ratio in the Pelagos Sanctuary and compared it with the ratio of 15 Mediterranean Sea GSAs (Fig.1). The Pelagos Sanctuary showed ratio values which were significantly larger than those predicted in the Alboran Sea (GSA 1), Algeria (GSA 2), Balearic Islands (GSA 3), Northern Spain and Gulf of Lion (GSA 4) and Aegean Sea (GSA 14), while they were significantly lower than those in the Tyrrhenian Sea (GSA 6), Southern Sicily and Malta (GSA 9), and the Northern Levant Sea (GSA 16). No significant differences were found with other GSAs (Fig. 4b).

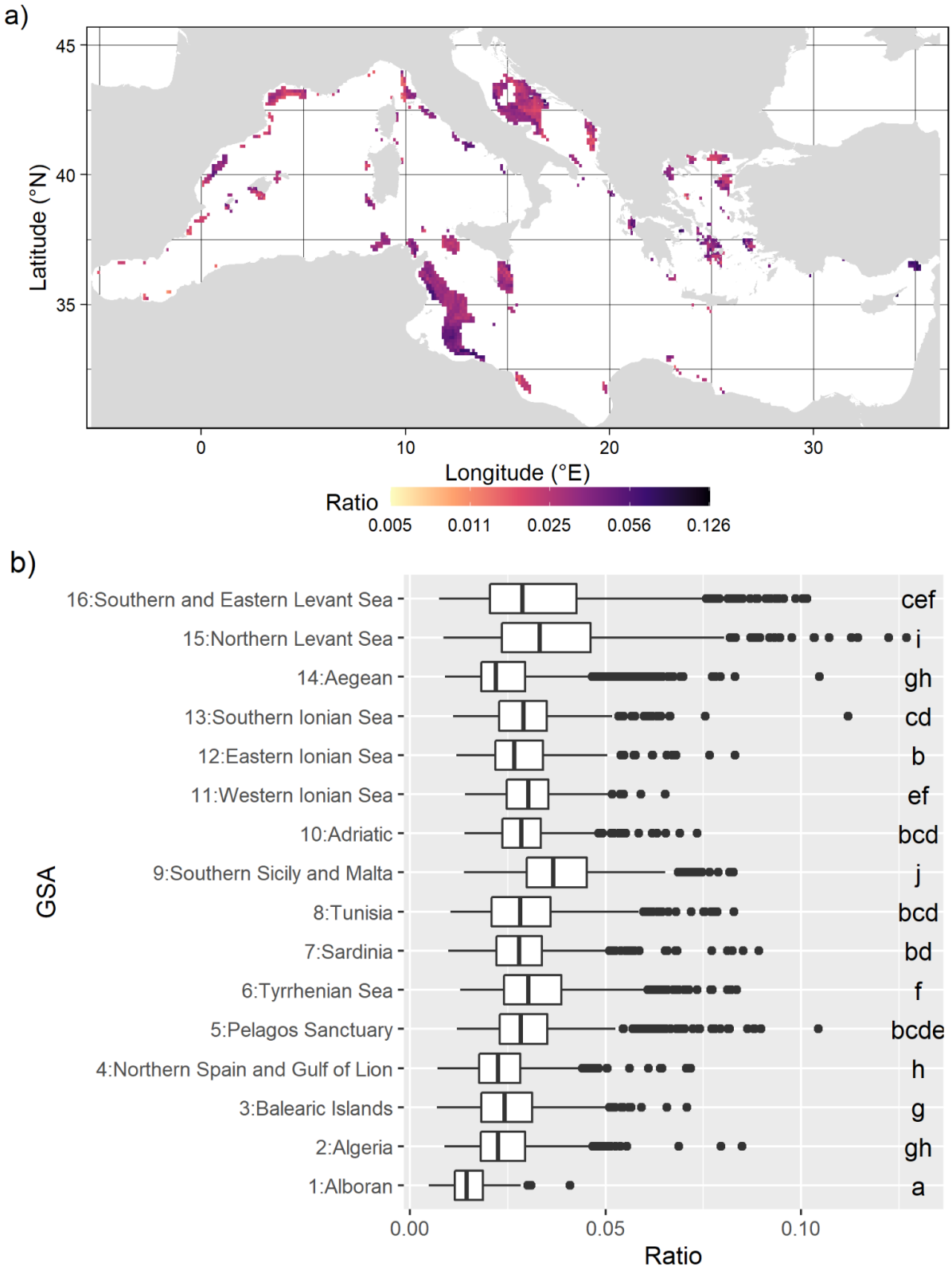

429

430 **<u>Figure 4 : Application of plastic to zooplankton ratio to two case studies :</u>**a) Plastic to

431 zooplankton ratio for plastic debris of size between 0.33—5 mm, showed only in

correspondence with the hotspots of small pelagic fish (defined as the locations with a biomass larger than the 90th percentile), b) boxplot of ratio values in the Pelagos Sanctuary and in 15 Mediterranean GSAs (shown in Fig. 1, MM 4). The letters on top of each box display pairwise wilcoxon test results.

IV. Discussion

4.1. Zooplankton distribution in the Mediterranean Sea and its drivers[7][8][9][10][11]

Zooplankton abundance was boosted by eddy presence, even if no clear preference for cyclones or anticyclones was detected. This was in accordance with previous studies finding large zooplankton concentration in eddies (Chambault et al., 2019; Godø et al., 2012; Riandey et al., 2005). Temperature played an important role in zooplankton abundances which decreased when temperature increased. This is because temperature affects the mixed layer depth (MLD) (D'Ortenzio et al., 2005). MLD governs the availability of nutrients and light, which are essential for phytoplankton, the primary food source for zooplankton. In regions with higher temperatures, such as the Levantine Basin, the MLD is relatively shallow (due to a low mixing in winter and a strong stratification in summer): this hampers nutrient supply to the phytoplankton, and in turn inhibits zooplankton growth; conversely, in the western basin, colder, the MLD is deeper, boosting biological activity (D'Ortenzio et al., 2005). High zooplankton abundance in coastal regions can also be attributed to phytoplankton blooms occurring near highly populated coasts, subject to terrigenous and river inputs in nutrients (Siokou-Frangou et al., 2010).

Frontal converging regions (identified through backward FTLE) were positively correlated with

455 zooplankton abundance. This is in coherence with previous studies highlighting the
456 importance of these features for mid trophic levels and, in general, the whole trophic chain
457 (Baudena et al., 2021; Chambault et al., 2017; d'Ovidio et al., 2010; Della Penna et al., 2015).
458 The negative correlation found with diverging zones (identified through forward FTLE and
459 divergence) suggest that these structures, even if fostering primary production, hamper
460 zooplankton concentration, possibly by spreading it away.
461 Notably, the pattern of zooplankton abundance over the whole Mediterranean was in
462 agreement with the average zooplankton mass in June–November 2014 obtained by the
463 Seapodym model (Lehodey et al., 2010; Fig. S11): the western Mediterranean showed larger
464 values than the eastern Mediterranean; the largest values were predicted in the northern
465 Adriatic Sea and in the Algerian and Alboran basins both by our projection and by the
466 Seapodym model. Differences could be explained by the fact that we used zooplankton
467 abundance (in N/km^2) while Seapodym provided zooplankton mass, and by the different
468 methodological approaches.
469
470 **4.2. Plastic debris distribution in the Mediterranean Sea and its drivers**
471
472 Plastic debris concentration obtained from the projections was lower in regions characterised
473 by strong currents and turbulence. This was confirmed by the decreasing relationship found
474 between plastic debris and kinetic energy (50 % of the variance), TKE, and FTLE calculated
475 both forward and backward in time (Fig. 2d). The positive relationship found with nitrates, a
476 proxy for land-based pollution (e.g. river mouths or cities), indicated that plastic debris
477 abundance was linked with coastal sources. This suggests that plastic debris is released mainly
478 from coastal sources, in coherence with previous studies (Baudena et al., 2022; Liubartseva

et al., 2018), where less energetic features are found. When plastic debris moves offshore, turbulent activity and currents mix it, lowering plastic abundance. This is corroborated by the slightly negative relationship with FTLE calculated both forward and backward in time: plastic debris may be attracted by frontal converging regions but then spread away.

The projection of plastic concentration does not show regions of strong plastic accumulation. This is in coherence with previous studies (Baudena et al., 2022; Liubartseva et al., 2018), which attributed this lack to the strong spatio-temporal variability of Mediterranean currents. The plastic concentration pattern we obtained was similar to the one reported by (Liubartseva et al., 2018) despite the different methodological approach (a Lagrangian tracking model). Higher concentrations of plastic debris were found in the northern Adriatic and (GSA 10) in the Balearic and northern Spain Sea (GSAs 3 and 4) and in the Levantine Basin (GSAs 15 and 16). Lower concentrations were found in the central part of the Eastern Mediterranean (GSAs 14—16), in the Bomba Gulf (Southern part of GSA 13), and in the Alboran Sea (GSA 1). A larger concentration was predicted in the Cilician basin (GSA 15) and in a portion of the Gulf of Lion (GSA 4) by Liubartseva et al. (2018) model, likely driven by the nearby presence of coastal plastic sources. This result provides evidence of the soundness of the pattern we obtained.

Our model predicted a total of $4 \cdot 10^{11}$ plastic debris floating at the surface of the Mediterranean Sea. This value was in agreement with the results from (Pedrotti et al., 2022); $6 \cdot 10^{11}$, confidence interval $4—14 \cdot 10^{11}$). The difference may be explained by the fact that our model predicted the plastic debris concentration over the entire basin and not only at the location of the Tara Mediterranean Expedition stations.

In general, plastic models had better estimations than zooplankton models. This may be due to the relatively easier description of plastic dynamics rather than zooplankton abundance, which is driven by complex biological and ecological processes including growth, predation,

503 competition or behaviour including vertical migrations (Queré et al., 2005).

504

505 **4.3. Plastic to zooplankton ratio and wildlife exposure**

506

507 The plastic and zooplankton projections allowed us to calculate the plastic to zooplankton
508 ratio at the Mediterranean Sea scale. This ratio ranged approximately between 0.005 (i.e., 5
509 plastic debris every 1000 zooplankton organisms) and 0.100 (i.e., 100 plastic debris every
510 1000 zooplankton organisms) throughout the whole basin.
511 Our results on the risk of plastic ingestion for small pelagic fish suggested that they could
512 ingest large amounts of debris. Indeed, the ratio of plastic to zooplankton was moderate to
513 high in the two larger pelagic fish hotspots, located in the Gulf of Gabès (GSA 8) and in the
514 Adriatic Sea (GSA 10). This is of particular concern since both regions are heavily exploited by
515 fishing industries (Colloca et al., 2017). While we could not explicitly observe an ingestion of
516 plastic debris by small pelagic fish in situ, previous studies reported microplastic presence in
517 the stomach content of at least 87 fish species in the Mediterranean Sea (Habib et al., 2021),
518 many of them being commercially important (Jâms et al., 2020; Renzi et al., 2019).
519 The Pelagos Sanctuary showed plastic to zooplankton ratio values (0.031±0.014) significantly
520 larger than all the GSAs in the Western Mediterranean, with the exclusion of the Tyrrhenian
521 Sea, and which were comparable to several GSAs across the basin. This value was similar to
522 the average plastic to zooplankton ratio obtained in the northwestern Mediterranean by
523 Pedrotti et al., (2016) (2016; 0.03 ±1.40). These results highlight the potential ingestion of
524 plastic debris by whales in this region. Fossi et al., (2012) recorded phthalates (a main
525 constituent of plastic) in fin whale *Balaenoptera physalus* blubber, showing that they could
526 consume plastic debris directly or indirectly from water and plankton. Hence, these mammals,

among the largest filter feeders in the world and adapted to absorbing large quantities of prey in a single mouthful, are threatened in one of their main feeding areas which is heavily contaminated.

We stress that the latter cases are just two examples of how the plastic to zooplankton ratio can be used to estimate the threat represented by plastic debris on marine biota and, ultimately, on human health (Bhuyan et al., 2022). Several other applications are possible, including the study of marine protected areas (Soto-Navarro et al., 2021), fishery grounds (Colloca et al., 2017), or specific regional analyses, also unravelling the origin of the plastic debris (Liubartseva et al., 2019).

4.4. Limits

The present study is not a mechanistic understanding of plastic debris ingestion by small pelagic fish. Zooplankton communities and their quality as food supply for predators were not assessed. Feuilloley et al. (2022), using a long time series of zooplankton observations in the northwestern Mediterranean, showed that changes in zooplankton composition, size, and density may impact higher trophic levels, such as the fitness of small pelagic fish. Results should be considered cautiously as both plastic and zooplankton were averaged over 6 months in the same year (June—November 2014). We only analysed surface data, while zooplankton organisms live in the whole water column and several species have a diel vertical migration.

It was not possible to identify a value of plastic to zooplankton ratio over which the risk of plastic ingestion could be considered high, as no studies have investigated this question to date. A possible choice would be the percentile of the ratio distribution over the

Mediterranean Sea. However, as the plastic pollution is expected to increase in the future (Borrelle et al., 2020; Lau et al., 2020), so will the ratio. Further studies are needed on this issue.

Multiple caveats are associated with the use of statistical approaches in a dynamic environment: i) they did not allow us to establish a causal relationship between plastic/zooplankton abundances and environment; ii) they have limited capacities to extrapolate in space and time (Guisan and Thuiller, 2005; Ralston and Moore, 2020; Yates et al., 2018). However, these approaches have proved to be useful, valuable, and cost-effective tools to quantify plastic/zooplankton distribution, especially in data-poor areas (Fabri-Ruiz et al., 2019; Guillaumot et al., 2019).

V. Conclusions

All in all, our findings showed that plastic debris is widespread in the Mediterranean Sea, with a number of debris in a similar order of magnitude than zooplankton organisms across the entire basin. This highlights the potential stress induced by this invasive element on the marine ecosystems, and the necessity of further research efforts on these questions. Further samplings of plastic debris and zooplankton organisms are needed, with larger spatio-temporal resolutions and water column observations. In addition, the understanding of the interaction between top predators, fish, and lower trophic levels in the presence of plastic will be crucial to correctly assess the threat encountered and to design mitigation strategies.

Acknowledgments and funding

We thank the commitment of the following institutions: CNRS, Sorbonne University, LOV. The Tara Ocean Foundation and its founders and sponsors: agnès b.®, Etienne Bourgois, the Veolia Environment Foundation, Lorient Agglomeration, Serge Ferrari, the Foundation Prince Albert II of Monaco, IDEC, the "Tara" schooner, crews and teams. We thank MERCATOR-CORIOLIS and ACRI-ST for providing daily satellite data during the expedition. We are also grateful to the French Ministry of Foreign Affairs for supporting the expedition and to the countries that graciously granted sampling permission. The authors are grateful to Enrico Ser-Giacomi for his helpful advice on the design of the research. This study was financed by the French Ministry for Ecological Transition (MTES) who supported a post-doctoral fellowship for Salome Fabri-Ruiz and EU H2020 LABPLAS project under the grant agreement (ID: 101003954), DOI: 10.3030/101003954.

Data availability

All the data necessary to produce the figures of the Main Text, i.e. the plastic and zooplankton abundances calculated over the whole Mediterranean Sea, the plastic to zooplankton ratio, the partition of the different GSAs used, as well as the climatology of the small pelagic fish biomass are available at https://doi.org/10.5281/zenodo.7076175. The in situ plastic concentrations are available at https://doi.org/ 10.5281/zenodo.5538237. The velocity field used to calculate the Lagrangian diagnostics are available on the E.U. Copernicus Marine

Environment Service Information website (CMEMS, http://marine.copernicus.eu/).

References

Aretoulaki, E., Ponis, S., National Technical University Athens, Plakas, G., National Technical University Athens, Agalianos, K., National Technical University Athens,

2021. Marine plastic littering: a review of socio economic impacts. J. Sustain. Sci. Manag. 16, 276–300. https://doi.org/10.46754/jssm.2021.04.019

Babak, N., 2015. usdm: Uncertainty analysis for species distribution models. R package version 1.1-15.

Baudena, A., Ser-Giacomi, E., D'Onofrio, D., Capet, X., Cotté, C., Cherel, Y., D'Ovidio, F., 2021. Fine-scale structures as spots of increased fish concentration in the open ocean. Sci. Rep. 11, 15805. https://doi.org/10.1038/s41598-021-94368-1

Baudena, A., Ser-Giacomi, E., Jalón-Rojas, I., Galgani, F., Pedrotti, M.L., 2022. The streaming of plastic in the Mediterranean Sea. Nat. Commun. 13, 2981. https://doi.org/10.1038/s41467-022-30572-5

Baudena, A., Ser-Giacomi, E., López, C., Hernández-García, E., d'Ovidio, F., 2019. Crossroads of the mesoscale circulation. J. Mar. Syst. 192, 1–14. https://doi.org/10.1016/j.jmarsys.2018.12.005

Beaumont, N.J., Aanesen, M., Austen, M.C., Börger, T., Clark, J.R., Cole, M., Hooper, T., Lindeque, P.K., Pascoe, C., Wyles, K.J., 2019. Global ecological, social and economic impacts of marine plastic. Mar. Pollut. Bull. 142, 189–195. https://doi.org/10.1016/j.marpolbul.2019.03.022

Bhuyan, Md.S., Rashed-Un-Nabi, Md., Alam, Md.W., Islam, Md.N., Cáceres-Farias, L., Bat, L., Musthafa, M.S., Senapathi, V., Chung, S.Y., Núñez, A.A., 2022. Environmental and Morphological Detrimental Effects of Microplastics on Marine Organisms to Human Health (preprint). In Review. https://doi.org/10.21203/rs.3.rs-1290795/v1[12][13]

Borrelle, S.B., Ringma, J., Law, K.L., Monnahan, C.C., Lebreton, L., McGivern, A., Murphy, E., Jambeck, J., Leonard, G.H., Hilleary, M.A., Eriksen, M., Possingham, H.P., De Frond, H., Gerber, L.R., Polidoro, B., Tahir, A., Bernard, M., Mallos, N., Barnes, M., Rochman, C.M., 2020. Predicted growth in plastic waste exceeds efforts to mitigate plastic pollution. Science 369, 1515–1518. https://doi.org/10.1126/science.aba3656

Bray, L., Digka, N., Tsangaris, C., Camedda, A., Gambaiani, D., de Lucia, G.A., Matiddi, M.,

Miaud, C., Palazzo, L., Pérez-del-Olmo, A., Raga, J.A., Silvestri, C., Kaberi, H., 2019. Determining suitable fish to monitor plastic ingestion trends in the Mediterranean Sea. Environ. Pollut. 247, 1071–1077. https://doi.org/10.1016/j.envpol.2019.01.100

Chambault, P., Baudena, A., Bjorndal, K.A., Santos, M.A.R., Bolten, A.B., Vandeperre, F., 2019. Swirling in the ocean: Immature loggerhead turtles seasonally target old anticyclonic eddies at the fringe of the North Atlantic gyre. Prog. Oceanogr. 175, 345–358. https://doi.org/10.1016/j.pocean.2019.05.005

Chambault, P., Roquet, F., Benhamou, S., Baudena, A., Pauthenet, E., de Thoisy, B., Bonola, M., Dos Reis, V., Crasson, R., Brucker, M., Le Maho, Y., Chevallier, D., 2017. The Gulf Stream frontal system: A key oceanographic feature in the habitat selection of the leatherback turtle? Deep Sea Res. Part Oceanogr. Res. Pap. 123, 35–47. https://doi.org/10.1016/j.dsr.2017.03.003

Chen, T., Guestrin, C., 2016. XGBoost: A Scalable Tree Boosting System, in: Proceedings of the 22nd ACM SIGKDD International Conference on Knowledge Discovery and Data Mining. Presented at the KDD '16: The 22nd ACM SIGKDD International Conference on Knowledge Discovery and Data Mining, ACM, San Francisco California USA, pp. 785–794. https://doi.org/10.1145/2939672.2939785

Chen, T., He, T., Benesty, M., Khotilovich, V., Tang, Y., Cho, H., Chen, K., 2015. Xgboost: extreme gradient boosting. R Package Version 04-2 1, 1–4.

Cole, M., Lindeque, P., Halsband, C., Galloway, T.S., 2011. Microplastics as contaminants in the marine environment: A review. Mar. Pollut. Bull. 62, 2588–2597. https://doi.org/10.1016/j.marpolbul.2011.09.025

Coll, M., Piroddi, C., Steenbeek, J., Kaschner, K., Ben Rais Lasram, F., Aguzzi, J., Ballesteros, E., Bianchi, C.N., Corbera, J., Dailianis, T., Danovaro, R., Estrada, M., Froglia, C., Galil, B.S., Gasol, J.M., Gertwagen, R., Gil, J., Guilhaumon, F., Kesner-Reyes, K., Kitsos, M.-S., Koukouras, A., Lampadariou, N., Laxamana, E., López-Fé de la Cuadra, C.M., Lotze, H.K., Martin, D., Mouillot, D., Oro, D., Raicevich, S., Rius-Barile, J., Saiz-Salinas, J.I., San Vicente, C., Somot, S., Templado, J., Turon, X.,

678 Vafidis, D., Villanueva, R., Voultsiadou, E., 2010. The Biodiversity of the
679 Mediterranean Sea: Estimates, Patterns, and Threats. PLoS ONE 5, e11842.
680 https://doi.org/10.1371/journal.pone.0011842
681 Collignon, A., Hecq, J.-H., Galgani, F., Collard, F., Goffart, A., 2014. Annual variation in
682 neustonic micro- and meso-plastic particles and zooplankton in the Bay of Calvi
683 (Mediterranean–Corsica). Mar. Pollut. Bull. 79, 293–298.
684 https://doi.org/10.1016/j.marpolbul.2013.11.023
685 Colloca, F., Scarcella, G., Libralato, S., 2017. Recent Trends and Impacts of Fisheries
686 Exploitation on Mediterranean Stocks and Ecosystems. Front. Mar. Sci. 4, 244.
687 https://doi.org/10.3389/fmars.2017.00244
688 Cózar, A., Sanz-Martín, M., Martí, E., González-Gordillo, J.I., Ubeda, B., Gálvez, J.Á.,
689 Irigoien, X., Duarte, C.M., 2015. Plastic Accumulation in the Mediterranean Sea.
690 PLOS ONE 10, e0121762. https://doi.org/10.1371/journal.pone.0121762
691 Croll, D.A., Tershy, B.R., Newton, K.M., de Vos, A., Hazen, E., Goldbogen, J.A., 2018. Filter
692 feeding, in: Encyclopedia of Marine Mammals. Elsevier, pp. 363–368.
693 d'Ovidio, F., De Monte, S., Alvain, S., Dandonneau, Y., Lévy, M., 2010. Fluid dynamical
694 niches of phytoplankton types. Proc. Natl. Acad. Sci. 107, 18366–18370.
695 https://doi.org/10.1073/pnas.1004620107
696 d'Ovidio, F., Della Penna, A., Trull, T.W., Nencioli, F., Pujol, M.-I., Rio, M.-H., Park, Y.-H.,
697 Cotté, C., Zhou, M., Blain, S., 2015. The biogeochemical structuring role of horizontal
698 stirring: Lagrangian perspectives on iron delivery downstream of the Kerguelen
699 Plateau. Biogeosciences 12, 5567–5581. https://doi.org/10.5194/bg-12-5567-2015
700 d'Ovidio, F., Fernández, V., Hernández-García, E., López, C., 2004. Mixing structures in the
701 Mediterranean Sea from finite-size Lyapunov exponents: Mixing structures in the
702 Mediterranean sea. Geophys. Res. Lett. 31, n/a-n/a.
703 https://doi.org/10.1029/2004GL020328
704 Della Penna, A., De Monte, S., Kestenare, E., Guinet, C., d'Ovidio, F., 2015. Quasi-
705 planktonic behavior of foraging top marine predators. Sci. Rep. 5, 18063.

https://doi.org/10.1038/srep18063

Dormann, C.F., Elith, J., Bacher, S., Buchmann, C., Carl, G., Carré, G., Marquéz, J.R.G., Gruber, B., Lafourcade, B., Leitão, P.J., Münkemüller, T., McClean, C., Osborne, P.E., Reineking, B., Schröder, B., Skidmore, A.K., Zurell, D., Lautenbach, S., 2013. Collinearity: a review of methods to deal with it and a simulation study evaluating their performance. Ecography 36, 27–46. https://doi.org/10.1111/j.1600-0587.2012.07348.x

D'Ortenzio, F., Iudicone, D., de Boyer Montegut, C., Testor, P., Antoine, D., Marullo, S., Santoleri, R., Madec, G., 2005. Seasonal variability of the mixed layer depth in the Mediterranean Sea as derived from in situ profiles: mixed layer depth over the Mediterranean. Geophys. Res. Lett. 32, n/a-n/a. https://doi.org/10.1029/2005GL022463

Doyle, M.J., Watson, W., Bowlin, N.M., Sheavly, S.B., 2011. Plastic particles in coastal pelagic ecosystems of the North-East Pacific ocean. Mar. Environ. Res. 71, 41–52. https://doi.org/10.1016/j.marenvres.2010.10.001

Fabri-Ruiz, S., Danis, B., David, B., Saucède, T., 2019. Can we generate robust species distribution models at the scale of the Southern Ocean? Divers. Distrib. 25, 21–37. https://doi.org/10.1111/ddi.12835

Feuilloley, G., Fromentin, J.-M., Saraux, C., Irisson, J.-O., Jalabert, L., Stemmann, L., 2022. Temporal fluctuations in zooplankton size, abundance, and taxonomic composition since 1995 in the North Western Mediterranean Sea. ICES J. Mar. Sci. 79, 882–900. https://doi.org/10.1093/icesjms/fsab190

Fitzpatrick, M.C., Lachmuth, S., Haydt, N.T., 2021. The ODMAP protocol: a new tool for standardized reporting that could revolutionize species distribution modeling. Ecography 44, 1067–1070. https://doi.org/10.1111/ecog.05700

Fossi, M.C., Coppola, D., Baini, M., Giannetti, M., Guerranti, C., Marsili, L., Panti, C., de Sabata, E., Clò, S., 2014. Large filter feeding marine organisms as indicators of microplastic in the pelagic environment: The case studies of the Mediterranean

basking shark (*Cetorhinus maximus*) and fin whale (*Balaenoptera physalus*). Mar. Environ. Res. 100, 17–24. https://doi.org/10.1016/j.marenvres.2014.02.002

Fossi, M.C., Panti, C., Guerranti, C., Coppola, D., Giannetti, M., Marsili, L., Minutoli, R., 2012. Are baleen whales exposed to the threat of microplastics? A case study of the Mediterranean fin whale (*Balaenoptera physalus*). Mar. Pollut. Bull. 64, 2374–2379. https://doi.org/10.1016/j.marpolbul.2012.08.013

Friedman, J.H., 2001. Greedy function approximation: a gradient boosting machine. Ann. Stat. 1189–1232.

Galgani, F., Claro, F., Depledge, M., Fossi, C., 2014. Monitoring the impact of litter in large vertebrates in the Mediterranean Sea within the European Marine Strategy Framework Directive (MSFD): Constraints, specificities and recommendations. Mar. Environ. Res. 100, 3–9. https://doi.org/10.1016/j.marenvres.2014.02.003

Garrido, S., Ben-Hamadou, R., Oliveira, P., Cunha, M., Chícharo, M., van der Lingen, C., 2008. Diet and feeding intensity of sardine *Sardina pilchardus*: correlation with satellite-derived chlorophyll data. Mar. Ecol. Prog. Ser. 354, 245–256. https://doi.org/10.3354/meps07201

Garrido, S., Marçalo, A., Zwolinski, J., van der Lingen, C., 2007. Laboratory investigations on the effect of prey size and concentration on the feeding behaviour of *Sardina pilchardus*. Mar. Ecol. Prog. Ser. 330, 189–199. https://doi.org/10.3354/meps330189

Gelman, A., Hill, J., 2006. Data Analysis Using Regression and Multilevel/Hierarchical Models. Cambridge University Press.

Gerigny, O., Brun, M., Fabri, M.C., Tomasino, C., Le Moigne, M., Jadaud, A., Galgani, F., 2019. Seafloor litter from the continental shelf and canyons in French Mediterranean Water: Distribution, typologies and trends. Mar. Pollut. Bull. 146, 653–666. https://doi.org/10.1016/j.marpolbul.2019.07.030

Gérigny, O., Pedrotti, M.-L., El Rakwe, M., Brun, M., Pavec, M., Henry, M., Mazeas, F., Maury, J., Garreau, P., Galgani, F., 2022. Characterization of floating microplastic contamination in the bay of Marseille (French Mediterranean Sea) and its impact on

zooplankton and mussels. Mar. Pollut. Bull. 175, 113353. https://doi.org/10.1016/j.marpolbul.2022.113353

Godø, O.R., Samuelsen, A., Macaulay, G.J., Patel, R., Hjøllo, S.S., Horne, J., Kaartvedt, S., Johannessen, J.A., 2012. Mesoscale Eddies Are Oases for Higher Trophic Marine Life. PLoS ONE 7, e30161. https://doi.org/10.1371/journal.pone.0030161

Gorsky, G., Ohman, M.D., Picheral, M., Gasparini, S., Stemmann, L., Romagnan, J.-B., Cawood, A., Pesant, S., Garcia-Comas, C., Prejger, F., 2010. Digital zooplankton image analysis using the ZooScan integrated system. J. Plankton Res. 32, 285–303. https://doi.org/10.1093/plankt/fbp124

Gove, J.M., Whitney, J.L., McManus, M.A., Lecky, J., Carvalho, F.C., Lynch, J.M., Li, J., Neubauer, P., Smith, K.A., Phipps, J.E., Kobayashi, D.R., Balagso, K.B., Contreras, E.A., Manuel, M.E., Merrifield, M.A., Polovina, J.J., Asner, G.P., Maynard, J.A., Williams, G.J., 2019. Prey-size plastics are invading larval fish nurseries. Proc. Natl. Acad. Sci. 116, 24143–24149. https://doi.org/10.1073/pnas.1907496116

Guillaumot, C., Artois, J., Saucède, T., Demoustier, L., Moreau, C., Eléaume, M., Agüera, A., Danis, B., 2019. Broad-scale species distribution models applied to data-poor areas. Prog. Oceanogr. 175, 198–207. https://doi.org/10.1016/j.pocean.2019.04.007

Guisan, A., Thuiller, W., 2005. Predicting species distribution: offering more than simple habitat models. Ecol. Lett. 8, 993–1009. https://doi.org/10.1111/j.1461-0248.2005.00792.x

Hernández-Carrasco, I., Orfila, A., Rossi, V., Garçon, V., 2018. Effect of small scale transport processes on phytoplankton distribution in coastal seas. Sci. Rep. 8, 8613. https://doi.org/10.1038/s41598-018-26857-9

Jâms, I.B., Windsor, F.M., Poudevigne-Durance, T., Ormerod, S.J., Durance, I., 2020. Estimating the size distribution of plastics ingested by animals. Nat. Commun. 11, 1594. https://doi.org/10.1038/s41467-020-15406-6

Kershaw, P.J., Turra, A., Galgani, F., 2019. Guidelines for the monitoring and assessment of plastic litter and microplastics in the ocean.

790 Lattin, G.L., Moore, C.J., Zellers, A.F., Moore, S.L., Weisberg, S.B., 2004. A comparison of
791 neustonic plastic and zooplankton at different depths near the southern California
792 shore. Mar. Pollut. Bull. 49, 291–294. https://doi.org/10.1016/j.marpolbul.2004.01.020
793 Lau, W.W.Y., Shiran, Y., Bailey, R.M., Cook, E., Stuchtey, M.R., Koskella, J., Velis, C.A.,
794 Godfrey, L., Boucher, J., Murphy, M.B., Thompson, R.C., Jankowska, E., Castillo
795 Castillo, A., Pilditch, T.D., Dixon, B., Koerselman, L., Kosior, E., Favoino, E.,
796 Gutberlet, J., Baulch, S., Atreya, M.E., Fischer, D., He, K.K., Petit, M.M., Sumaila,
797 U.R., Neil, E., Bernhofen, M.V., Lawrence, K., Palardy, J.E., 2020. Evaluating
798 scenarios toward zero plastic pollution. Science 369, 1455–1461.
799 https://doi.org/10.1126/science.aba9475
800 Le Bourg, B., Bănaru, D., Saraux, C., Nowaczyk, A., Le Luherne, E., Jadaud, A., Bigot, J.L.,
801 Richard, P., 2015. Trophic niche overlap of sprat and commercial small pelagic
802 teleosts in the Gulf of Lions (NW Mediterranean Sea). J. Sea Res. 103, 138–146.
803 https://doi.org/10.1016/j.seares.2015.06.011
804 Lefebvre, C., Saraux, C., Heitz, O., Nowaczyk, A., Bonnet, D., 2019. Microplastics FTIR
805 characterisation and distribution in the water column and digestive tracts of small
806 pelagic fish in the Gulf of Lions. Mar. Pollut. Bull. 142, 510–519.
807 https://doi.org/10.1016/j.marpolbul.2019.03.025
808 Liubartseva, S., Coppini, G., Lecci, R., 2019. Are Mediterranean Marine Protected Areas
809 sheltered from plastic pollution? Mar. Pollut. Bull. 140, 579–587.
810 https://doi.org/10.1016/j.marpolbul.2019.01.022
811 Liubartseva, S., Coppini, G., Lecci, R., Clementi, E., 2018. Tracking plastics in the
812 Mediterranean: 2D Lagrangian model. Mar. Pollut. Bull. 129, 151–162.
813 https://doi.org/10.1016/j.marpolbul.2018.02.019
814 Mansui, J., Darmon, G., Ballerini, T., van Canneyt, O., Ourmieres, Y., Miaud, C., 2020.
815 Predicting marine litter accumulation patterns in the Mediterranean basin: Spatio-
816 temporal variability and comparison with empirical data. Prog. Oceanogr. 182,
817 102268. https://doi.org/10.1016/j.pocean.2020.102268

818 Moore, C.J., Moore, S.L., Weisberg, S.B., Lattin, G.L., Zellers, A.F., 2002. A comparison of
819 neustonic plastic and zooplankton abundance in southern California's coastal waters.
820 Mar. Pollut. Bull. 44, 1035–1038. https://doi.org/10.1016/S0025-326X(02)00150-9
821 Morgado, C., Martins, A., Rosso, M., Moulins, A., Tepsich, P., 2017. Fin Whale Presence
822 and Distribution in the Pelagos Sanctuary: Temporal and Spatial Variability Along 2
823 Fixed-Line Transects Monitored in 2009-2013 14.
824 Moullec, F., Barrier, N., Drira, S., Guilhaumon, F., Hattab, T., Peck, M.A., Shin, Y.-J., 2022.
825 Using species distribution models only may underestimate climate change impacts
826 on future marine biodiversity. Ecol. Model. 464, 109826.
827 https://doi.org/10.1016/j.ecolmodel.2021.109826
828 Moullec, F., Barrier, N., Drira, S., Guilhaumon, F., Marsaleix, P., Somot, S., Ulses, C., Velez,
829 L., Shin, Y.-J., 2019a. An End-to-End Model Reveals Losers and Winners in a
830 Warming Mediterranean Sea. Front. Mar. Sci. 6, 345.
831 https://doi.org/10.3389/fmars.2019.00345
832 Moullec, F., Velez, L., Verley, P., Barrier, N., Ulses, C., Carbonara, P., Esteban, A., Follesa,
833 C., Gristina, M., Jadaud, A., Ligas, A., Díaz, E.L., Maiorano, P., Peristeraki, P.,
834 Spedicato, M.T., Thasitis, I., Valls, M., Guilhaumon, F., Shin, Y.-J., 2019b. Capturing
835 the big picture of Mediterranean marine biodiversity with an end-to-end model of
836 climate and fishing impacts. Prog. Oceanogr. 178, 102179.
837 https://doi.org/10.1016/j.pocean.2019.102179
838 Onink, V., Wichmann, D., Delandmeter, P., Sebille, E., 2019. The Role of Ekman Currents,
839 Geostrophy, and Stokes Drift in the Accumulation of Floating Microplastic. J.
840 Geophys. Res. Oceans 124, 1474–1490. https://doi.org/10.1029/2018JC014547
841 Pedrotti, M.L., Lombard, F., Baudena, A., Galgani, F., Elineau, A., Petit, S., Henry, M.,
842 Troublé, R., Reverdin, G., Ser-Giacomi, E., Kedzierski, M., Boss, E., Gorsky, G.,
843 2022. An integrative assessment of the plastic debris load in the Mediterranean Sea.
844 Sci. Total Environ. 838, 155958. https://doi.org/10.1016/j.scitotenv.2022.155958
845 Pedrotti, M.L., Petit, S., Elineau, A., Bruzaud, S., Crebassa, J.-C., Dumontet, B., Martí, E.,

Gorsky, G., Cózar, A., 2016. Changes in the Floating Plastic Pollution of the Mediterranean Sea in Relation to the Distance to Land. PLOS ONE 11, e0161581. https://doi.org/10.1371/journal.pone.0161581

Pennino, M.G., Bachiller, E., Lloret-Lloret, E., Albo-Puigserver, M., Esteban, A., Jadaud, A., Bellido, J.M., Coll, M., 2020. Ingestion of microplastics and occurrence of parasite association in Mediterranean anchovy and sardine. Mar. Pollut. Bull. 158, 111399. https://doi.org/10.1016/j.marpolbul.2020.111399

Picheral, M., Colin, S., Irisson, J.O., 2017. EcoTaxa, a tool for the taxonomic classification of images. URL Httpecotaxa Obs-Vlfr Fr.

Provencher, J.F., Ammendolia, J., Rochman, C.M., Mallory, M.L., 2019. Assessing plastic debris in aquatic food webs: what we know and don't know about uptake and trophic transfer. Environ. Rev. 27, 304–317. https://doi.org/10.1139/er-2018-0079

Queiros, Q., Fromentin, J.-M., Gasset, E., Dutto, G., Huiban, C., Metral, L., Leclerc, L., Schull, Q., McKenzie, D.J., Saraux, C., 2019. Food in the Sea: Size Also Matters for Pelagic Fish. Front. Mar. Sci. 6, 385. https://doi.org/10.3389/fmars.2019.00385

Ralston, D.K., Moore, S.K., 2020. Modeling harmful algal blooms in a changing climate. Harmful Algae 91, 101729. https://doi.org/10.1016/j.hal.2019.101729

Renzi, M., Specchiulli, A., Blašković, A., Manzo, C., Mancinelli, G., Cilenti, L., 2019. Marine litter in stomach content of small pelagic fishes from the Adriatic Sea: sardines (*Sardina pilchardus*) and anchovies (*Engraulis encrasicolus*). Environ. Sci. Pollut. Res. 26, 2771–2781. https://doi.org/10.1007/s11356-018-3762-8

Riandey, V., Champalbert, G., Carlotti, F., Taupier-Letage, I., Thibault-Botha, D., 2005. Zooplankton distribution related to the hydrodynamic features in the Algerian Basin (western Mediterranean Sea) in summer 1997. Deep Sea Res. Part Oceanogr. Res. Pap. 52, 2029–2048. https://doi.org/10.1016/j.dsr.2005.06.004

Rochman, C.M., Tahir, A., Williams, S.L., Baxa, D.V., Lam, R., Miller, J.T., Teh, F.-C., Werorilangi, S., Teh, S.J., 2015. Anthropogenic debris in seafood: Plastic debris and fibers from textiles in fish and bivalves sold for human consumption. Sci. Rep. 5,

14340. https://doi.org/10.1038/srep14340

Savoca, M.S., McInturf, A.G., Hazen, E.L., 2021. Plastic ingestion by marine fish is widespread and increasing. Glob. Change Biol. 27, 2188–2199. https://doi.org/10.1111/gcb.15533

Ser-Giacomi, E., Baudena, A., Rossi, V., Follows, M., Clayton, S., Vasile, R., López, C., Hernández-García, E., 2021. Lagrangian betweenness as a measure of bottlenecks in dynamical systems with oceanographic examples. Nat. Commun. 12, 4935. https://doi.org/10.1038/s41467-021-25155-9

Shin, Y.-J., Cury, P., 2001. Exploring fish community dynamics through size-dependent trophic interactions using a spatialized individual-based model. Aquat Living Resour 16. https://doi.org/10.1016/S0990-7440(01)01106-8

Shin, Y.-J., Shannon, L.J., Cury, P.M., 2004. Simulations of fishing effects on the southern Benguela fish community using an individual-based model: learning from a comparison with ECOSIM. Afr. J. Mar. Sci. 26, 95–114. https://doi.org/10.2989/18142320409504052

Simoncelli, S., Fratianni, C., Pinardi, N., Grandi, A., Drudi, M., Oddo, P., Dobricic, S., 2014. Mediterranean Sea physical reanalysis (MEDREA 1987–2015)(Version 1). Copernic Monit Env. Mar Serv CMEMS 10.

Siokou-Frangou, I., Christaki, U., Mazzocchi, M.G., Montresor, M., Ribera d'Alcalá, M., Vaqué, D., Zingone, A., 2010. Plankton in the open Mediterranean Sea: a review. Biogeosciences 7, 1543–1586. https://doi.org/10.5194/bg-7-1543-2010

Solomando, A., Pujol, F., Sureda, A., Pinya, S., 2022. Ingestion and characterization of plastic debris by loggerhead sea turtle, *Caretta caretta*, in the Balearic Islands. Sci. Total Environ. 826, 154159. https://doi.org/10.1016/j.scitotenv.2022.154159

Soto-Navarro, J., Jordá, G., Compa, M., Alomar, C., Fossi, M.C., Deudero, S., 2021. Impact of the marine litter pollution on the Mediterranean biodiversity: A risk assessment study with focus on the marine protected areas. Mar. Pollut. Bull. 165, 112169. https://doi.org/10.1016/j.marpolbul.2021.112169

Wei, T., Simko, V., Levy, M., Xie, Y., Jin, Y., Zemla, J., 2017. Package ‘corrplot.’ Statistician 56, e24.

Yates, K.L., Bouchet, P.J., Caley, M.J., Mengersen, K., Randin, C.F., Parnell, S., Fielding, A.H., Bamford, A.J., Ban, S., Barbosa, A.M., Dormann, C.F., Elith, J., Embling, C.B., Ervin, G.N., Fisher, R., Gould, S., Graf, R.F., Gregr, E.J., Halpin, P.N., Heikkinen, R.K., Heinänen, S., Jones, A.R., Krishnakumar, P.K., Lauria, V., Lozano-Montes, H., Mannocci, L., Mellin, C., Mesgaran, M.B., Moreno-Amat, E., Mormede, S., Novaczek, E., Oppel, S., Ortuño Crespo, G., Peterson, A.T., Rapacciuolo, G., Roberts, J.J., Ross, R.E., Scales, K.L., Schoeman, D., Snelgrove, P., Sundblad, G., Thuiller, W., Torres, L.G., Verbruggen, H., Wang, L., Wenger, S., Whittingham, M.J., Zharikov, Y., Zurell, D., Sequeira, A.M.M., 2018. Outstanding Challenges in the Transferability of Ecological Models. Trends Ecol. Evol. 33, 790–802. https://doi.org/10.1016/j.tree.2018.08.001

Zurell, D., Franklin, J., König, C., Bouchet, P.J., Dormann, C.F., Elith, J., Fandos, G., Feng, X., Guillera-Arroita, G., Guisan, A., Lahoz-Monfort, J.J., Leitão, P.J., Park, D.S., Peterson, A.T., Rapacciuolo, G., Schmatz, D.R., Schröder, B., Serra-Diaz, J.M., Thuiller, W., Yates, K.L., Zimmermann, N.E., Merow, C., 2020. A standard protocol for reporting species distribution models. Ecography 43, 1261–1277. https://doi.org/10.1111/ecog.04960

Supplementary Materials

ODMAP protocol:

Confounding plastic and plankton: risk assessment of plastic ingestion in the Mediterranean sea

– ODMAP Protocol –

Salomé Fabri-Ruiz, Alberto Baudena, Fabien Moullec, Fabien Lombard, Jean-Olivier Irisson, Maria-Luiza Pedrotti

2022-08-02

Overview

Authorship

Contact : salome.fabri.ruiz@ifremer.fr

<Study link>

Model objective

Model objective: Inference and explanation

Focal Taxon

Focal Taxon: Microplastic and zooplankton

Location

Location: Mediterranean Sea

Scale of Analysis

Spatial extent: -3.7, 34.7, 30.9, 45 (xmin, xmax, ymin, ymax)

Spatial resolution: ≈13-km

Temporal extent: June to November 2014

Temporal resolution: 6 months

Boundary: rectangle

Biodiversity data

Observation type: field survey

Response data type: counts

Explanatory variables

Explanatory variable types: Abiotic explanatory variables and Lagrangian diagnostics

Hypotheses

Hypotheses: Microplastic abundances are driven by water masses characteristics. Zooplankton abundances are driven by abiotic explanatory variables and water masses characteristics

Assumptions

Model assumptions: Species/Microplastic–environment equilibrium

Algorithms

Modelling techniques: Xgboost

Model complexity: As we want to explain abundances patterns, we used only one algorithm. Model parametrization was made using cross-validation procedure and minimise log-likelihood for Poisson regression

Model averaging: No

Workflow

Model workflow: add each steps here

Software

Software: R software and packages used : xgboost, ModelMetrics,usdm,corrplot, tidyverse, ggplot2

<Code availability>

<Data availability>

Data

Biodiversity data

Taxon names: Zooplankton and plastic (between 0.33 and 5 mm, between 0.33 and 1 mm, between 1 and 5 mm, and all sizes i.e. larger than 0.33 mm)

<Taxonomic reference system>

<Ecological level>

<Data sources>

Sampling design: Details about sampling plan of Tara expedition, temporal design : from June to November 2014, No nestedness

Sample size: Counts

Absence data: No absences data

Background data: No background data

Explanatory variables variables :

Table S1 : Physical and biogeochemical data extracted from Copernicus

Variable	Acronyms	Units	Initial spatial resolution	Spatial resolution used	Time period	Time resolution
Mean temperature	temp_mean	°C	0.0625° x 0.0625°	0.125°x 0.125°	06/2014 to 11/2014	Daily then 6 months averaged
Mean Salinity	sal_mean	Psu	0.0625° x 0.0625°	0.125°x 0.125°	06/2014 to 11/2014	Weekly then 6 months averaged
Mean Dissolved oxygen (O_2)	O2_mean	$mmol.m^{-3}$	0.0625° x 0.0625°	0.125°x 0.125°	06/2014 to 11/2014	Weekly then 6 months averaged
Mean Nitrate (NO_3)	NO3_mean	$mmol.m^{-3}$	0.0625° x 0.0625°	0.125°x 0.125°	06/2014 to 11/2014	Weekly then 6 months averaged
Mean Phosphate (PO_4)	PO4_mean	$mmol.m^{-3}$	0.0625° x 0.0625°	0.125°x 0.125°	06/2014 to 11/2014	Weekly then 6 months averaged

Table S2 : Summary of Lagrangian and Eulerian diagnostic parameters

Lagrangian variables	Acronyms	Units	Spatial Resolution	Time period	Time resolution	Advection time	Distance threshold (only for lppi)
Finite Time Lyapunov Exponents	ftle	$days^{-1}$	0.125°x0.125°	06/2014 to 11/2014		15, 30, 45	-
Betweenness	betw	adim.	0.125°x0.125°	06/2014 to 11/2014		15, 30, 45	-
Retention time	ret.time	days	0.125°x0.125°	06/2014 to 11/2014		-	-
Okubo Weiss	ow	s^{-2}	0.125°x0.125°	06/2014 to 11/2014		0	-
Vorticity	vort	s^{-1}	0.125°x0.125°	06/2014 to 11/2014		0	-
Divergence	div	s^{-1}	0.125°x0.125°	06/2014 to 11/2014		0,5, 10, 15, 20, 25, 30, 35, 40, 45, 50, 55, 60	-
Absolute velocity	vel.abs	m/s	0.125°x0.125°	06/2014 to 11/2014		-	-
Kinetic energy	kinNRJ	m^2/s^2	0.125°x0.125°	06/2014 to 11/2014		-	-
Turbulent Kinetic Energy	tke	m^2/s^2	0.125°x0.125°	06/2014 to 11/2014		-	-
Lagrangian Plastic	lppi	adim.	0.125°x0.125°	06/2014		0,5, 10, 15,	0.5°, 0.75°, 1°,

Pollution Index		to 11/2014	20, 25, 30, 35, 40, 45, 50, 55, 60	1.5°

Table S3 : Explanatory variables used in Xgboost models for each group

Group	Zooplankton	Plastic	Plastic
Size	between 0.33 and 1 mm, between 1 and 5 mm, between 0.33 and 5 mm, all sizes	between 0.33 and 1 mm, between 1 and 5 mm, between 0.33 and 5 mm	All sizes
Distance threshold for lppi calculation	-	0.5°, 0.75°, 1°, 1.5°	0.5°, 0.75°, 1°, 1.5°
Variables	temp_mean	NO3_mean	PO4_mean
	sal_mean	ftle45_B	NO3_mean
	NO3_mean	ftle45_F	ftle45_B
	ftle45_B	betw15	ftle45_F
	ftle45_F	tke	betw15
	tke	ow0	tke
	ow0	vort0	ow0
	vort0	div0	vort0
	div0	kinNRJ	div0
	kinNRJ	lppi with advection time = 0 days	kinNRJ
		lppi with advection time = 60 days	lppi with advection time = 0
			lppi with advection time = 60 days

Data sources: http://marine.copernicus.eu/services-portfolio/access-to-products/?option=com_csw&view=details&product_id=MEDSEA_REANALYSIS_PHYS_006_004

Spatial extent: -3.7, 34.7, 30.9, 45 (xmin, xmax, ymin, ymax)

Spatial resolution: ~13km

Coordinate reference system: WGS84

Temporal extent: From June to November 2016

Transfer data

Spatial extent: -3.7, 34.7, 30.9, 45 (xmin, xmax, ymin, ymax)

Spatial resolution: ~13km

Temporal extent: From June to November 2016

Model

Multicollinearity

Multicollinearity: Variance inflation factors in a stepwise procedure and Spearman pair-wise correlation test

Model settings

Table S4: Predictive performance for each size class and each distance threshold for plastic

Group	Distance threshold for lppi calculation	Size	R^2	Model selected
Plastic	0.5°	Between 1 and 5 mm	0.68	
Plastic	0.75°	Between 1 and 5 mm	0.68	
Plastic	1°	Between 1 and 5 mm	0.5	
Plastic	1.5°	Between 1 and 5 mm	0.7	x
Plastic	0.5°	Between 0.33 and 1 mm	0.7	
Plastic	0.75°	Between 0.33 and 1 mm	0.74	x
Plastic	1°	Between 0.33 and 1 mm	0.73	
Plastic	1.5°	Between 0.33 and 1 mm	0.73	
Plastic	0.5°	All size	0.78	x
Plastic	0.75°	All size	0.6	

Plastic	1°	All size	0.5	
Plastic	1.5°	All size	0.46	

1012

1013

1014

1015

1016

1017

1018

1019 **Table S5**: Best parameters estimated from calibration model for each categories

1020

			Model parameters			
Group	**Size**	**R^2**	**Trees**	**Maximum depth**	**Eta**	**Minimum child weight**
Zooplankton	Between 0.33 and 1 mm	0.66	719	2	0.4	1
Zooplankton	Between 1 and 5 mm	0.77	702	2	0.4	5
Zooplankton	All sizes (i.e. > 0.33 mm)	0.62	717	2	0.4	1
Plastic	Between 0.33 and 1 mm	0.73	625	2	0.4	5
Plastic	Between 1 and 5 mm	0.7	627	2	0.4	1
Plastic	All sizes (i.e. > 0.33 mm)	0.78	661	2	0.4	5

1021

1022

1023 **Model estimates**

1024 Coefficients: mean and standard deviation

1025 **Analysis and Correction of non-independence**

1026 Spatial autocorrelation: No

Assessment

Performance statistics

Performance on training data: log-likelihood for Poisson regression.

Performance to assess difference between observed and predicted abundances : R^2 and pearson correlation coefficient.

Plausibility check

Response shapes: partial dependence plots

Supplementary Figures

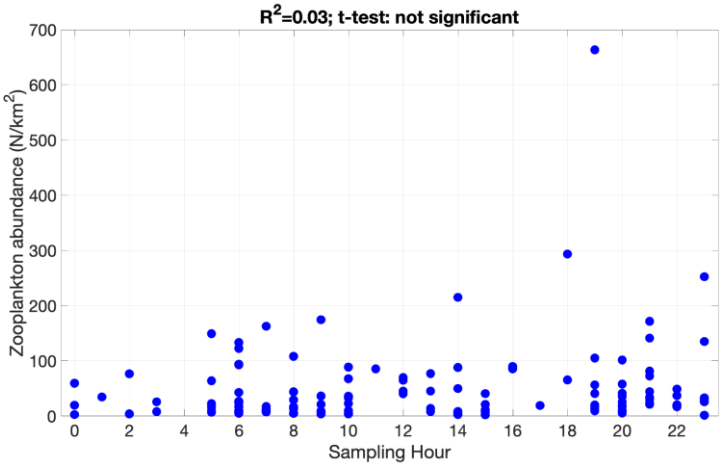

Figure S1: Zooplankton concentration (*y*-axis) as a function of the sampling hour (*x*-axis). R2=0.03, t-test not significant.

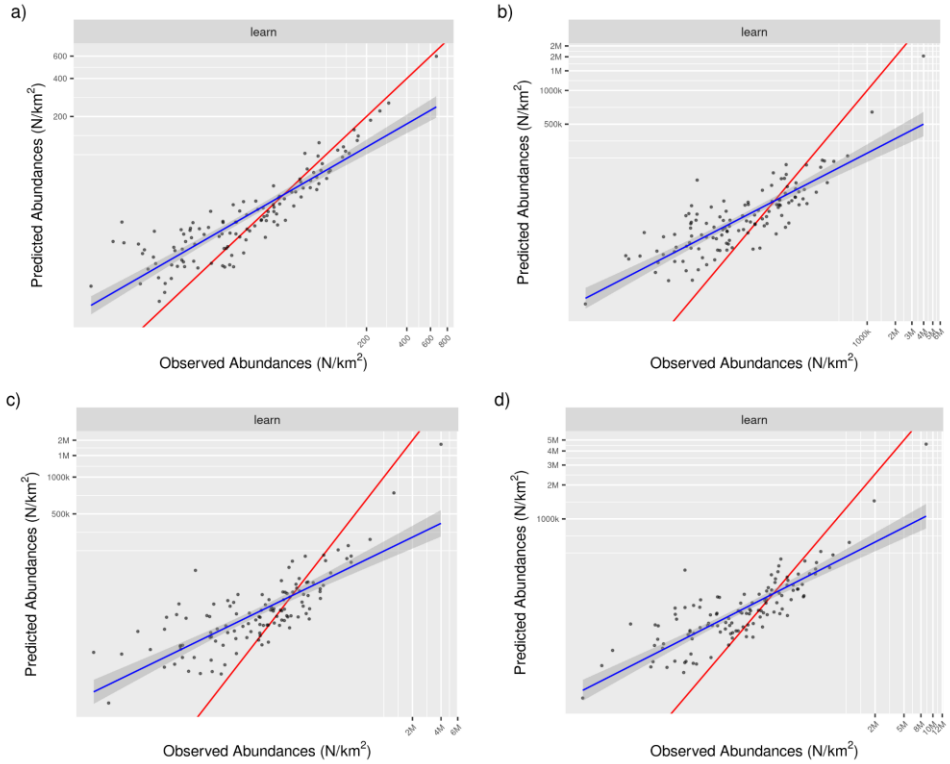

Figure s2 : Regression between predicted and observed abundance (blue line) for plastic a) between 0.33 and 5 mm, b) between 0.33 and 1 mm, c) between 1 and 5 mm and d) all sizes (i.e. > 0.33 mm). Red line is a line of equation 1:1, if points are on this line predicted values=observation. If points are above, predicted values are > observation and if below predicted values < observations

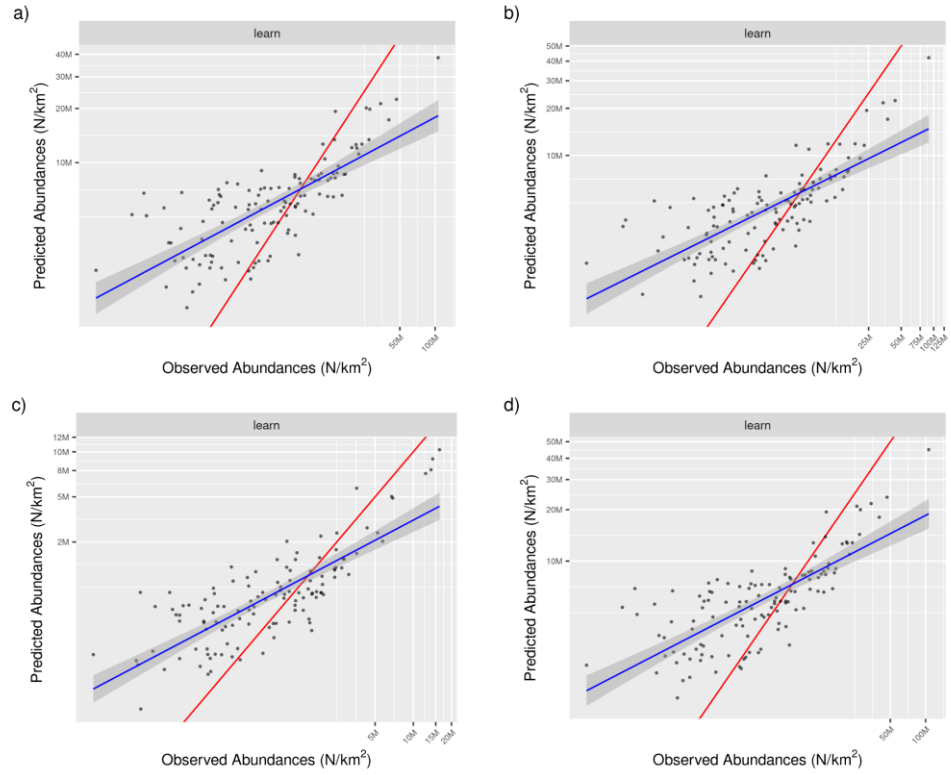

Figure S3 : Regression between predicted and observed abundance for zooplankton a) between 0.33 and 5 mm, b) between 0.33 and 1 mm, c) between 1 and 5 mm and d) all sizes (i.e. > 0.33 mm). Red line is a line of equation 1:1, if points are on this line predicted values=observation. If points are above, predicted values are > observation and if below predicted values < observations

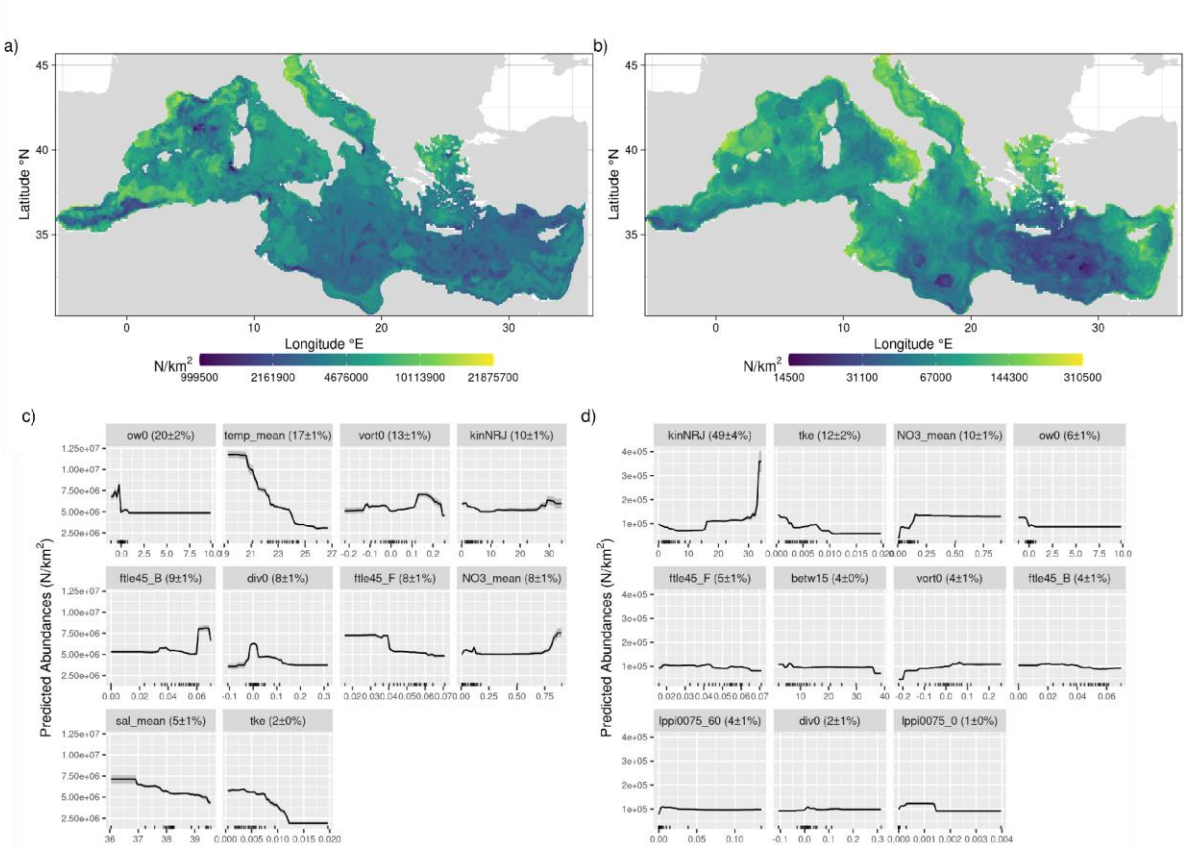

Figure S4: Spatial projection and partial dependence plot of zooplankton (panels a and c respectively) and plastic debris Between 0.33 and 1 mm (b and d respectively). oW0 = Okubo Weiss, kinNRJ = Kinetic Energy, temp_mean = mean temperature, NO3_mean = mean nitrate concentration, vort0 = vorticity , tke = Turbulent Kinetic Energy, ftle45_F = FTLE 45 days forward in time, ftle45_B = FTLE 45 days backward in time, div0 = Eulerian Divergence, betw15 = Betweenness at 15 days, sal_mean = mean salinity, lppi0075_60 = LPPI with distance threshold of 0.75° and 60 days backward in time, lppi0075_0 = LPPI with distance threshold of 0.75° and no advection

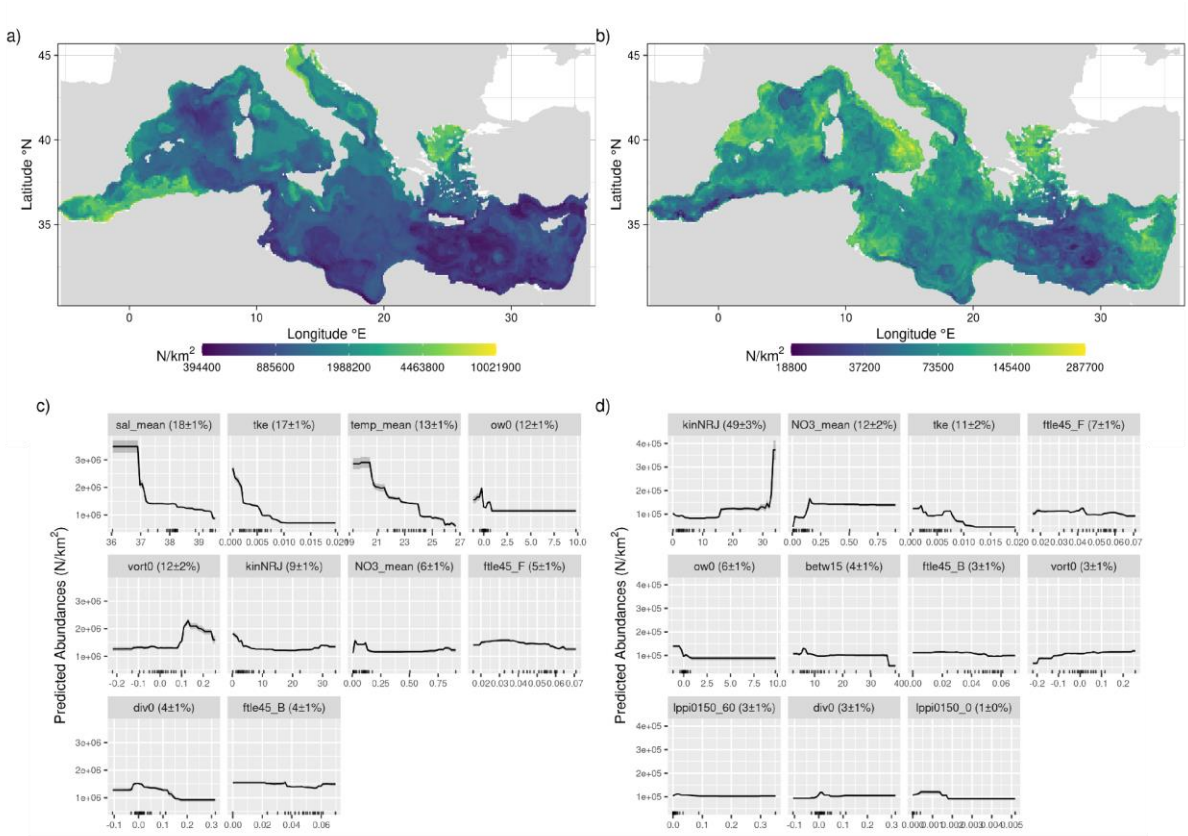

Figure S5: Spatial projection and partial dependence plot of zooplankton (a and c respectively) and plastic between 1 and 5 mm (b and d respectively). lppi0150_60 = LPPI with distance threshold of 1.5° and 60 days backward in time, lppi0150_0 = LPPI with distance threshold of 1.5° and no advection. The meaning of the other abbreviations in the partial dependence plots is reported in Fig. 2, Fig.S4, and in Table S1.

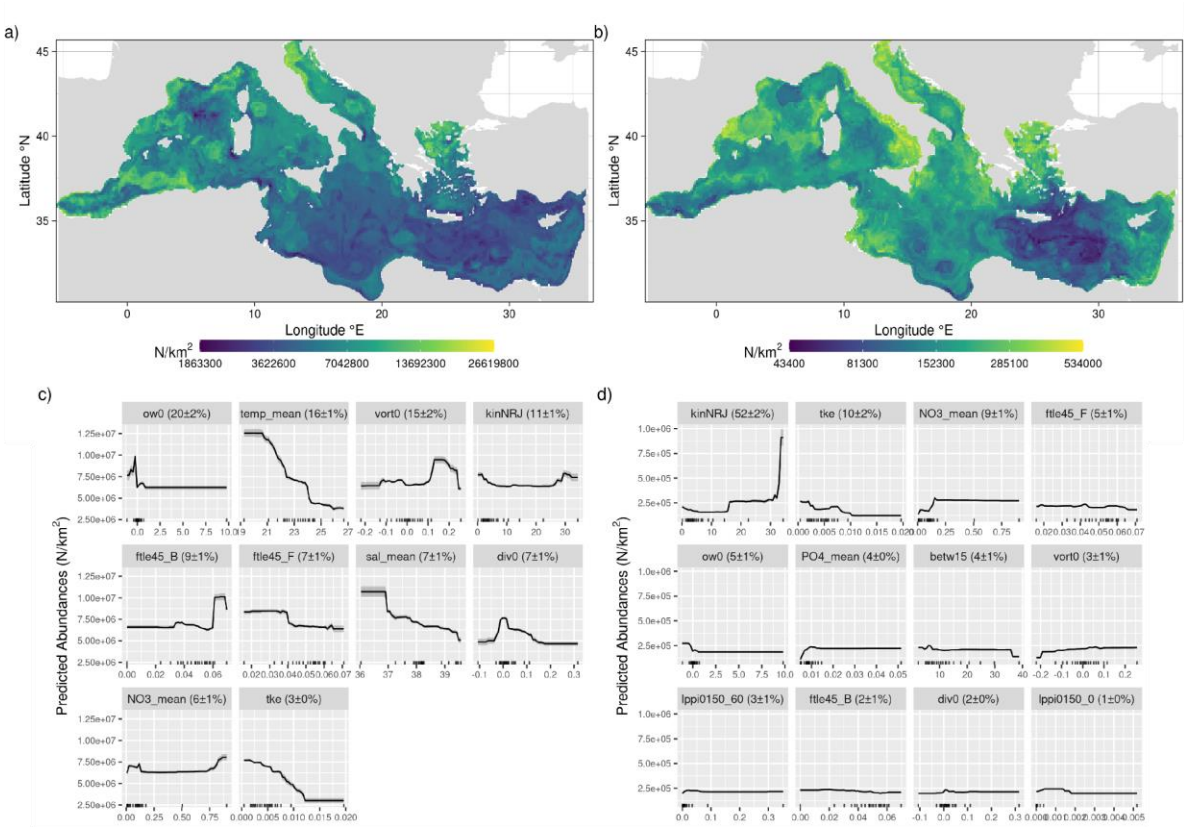

Figure S6: Spatial projection and partial dependence plot of zooplankton (a and c respectively) and plastic all size (b and d respectively). lppi0150_60 = LPPI with distance threshold of 1.5° and 60 days backward in time, lppi0150_0 = LPPI with distance threshold of 1.5° and no advection. The meaning of the other abbreviations in the partial dependence plots is reported in Fig. 2, Fig.S4, and in Table S1.

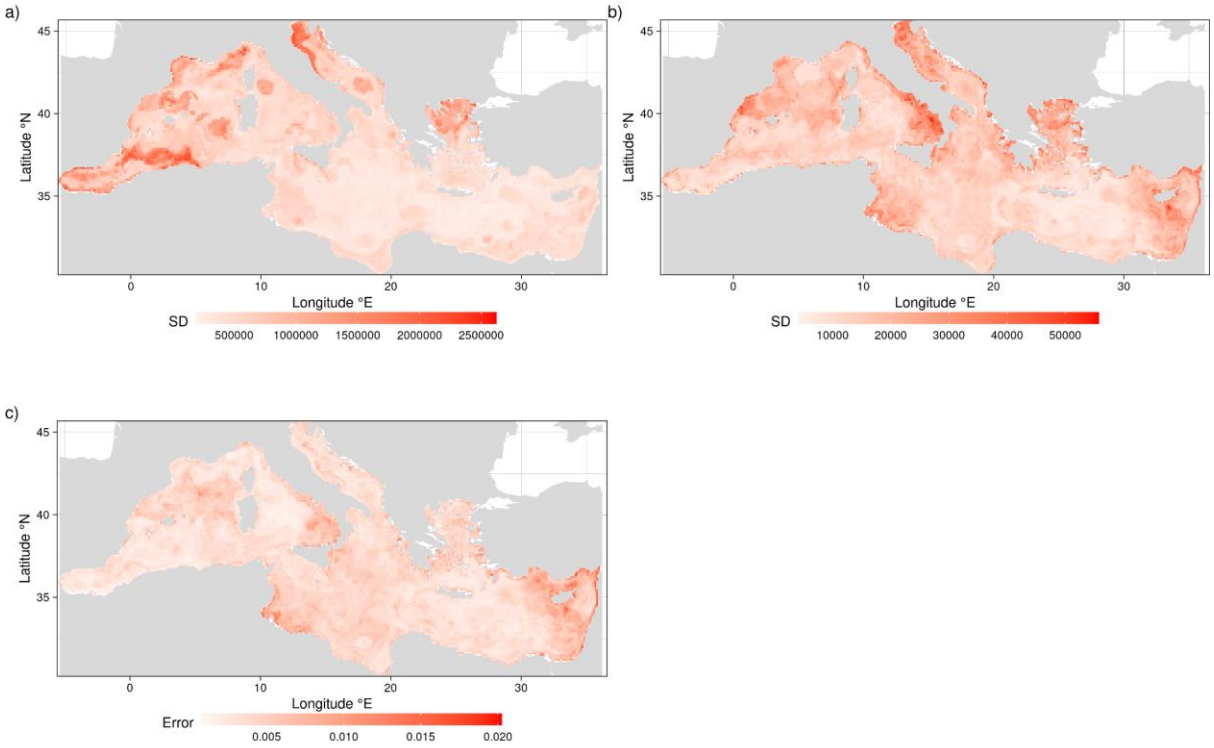

Figure S7: Standard deviation of the projection of a) zooplankton b) plastic debris concentration; c) plastic to zooplankton ratio (obtained from the error propagation using a and b panel values) for the size class between 0.33 and 5 mm.

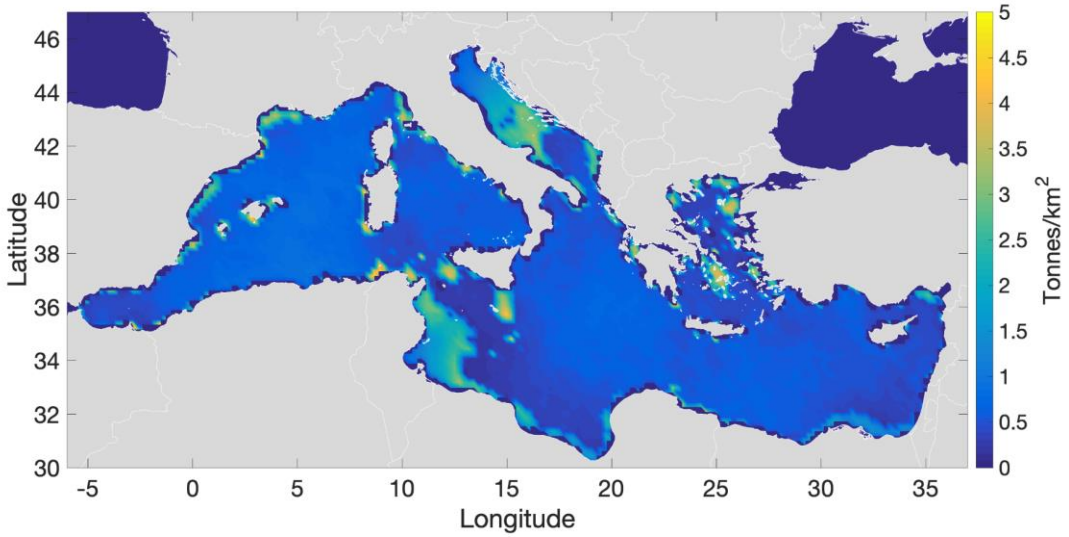

Figure S8: Small pelagic biomass in the Mediterranean Sea, calculated from the Osmose model (Materials and Methods)

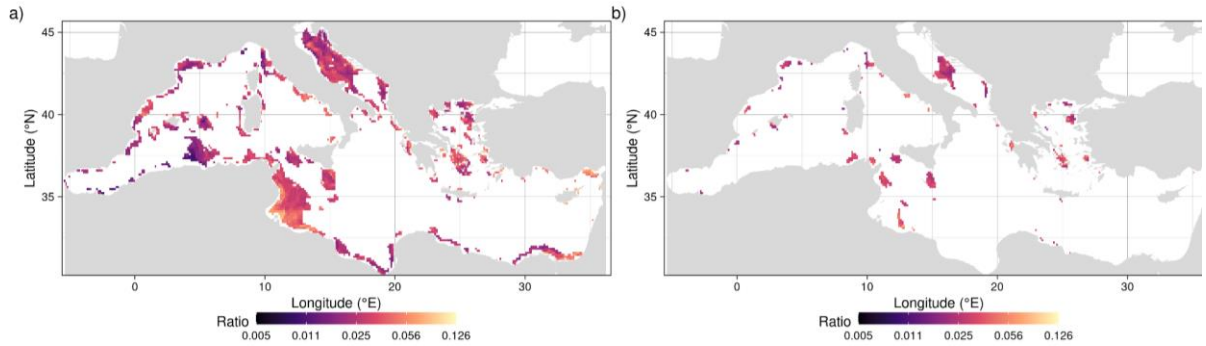

Figure S9 : Ratio zooplankton:plastic debris of size between 0.33 and 5 mm, showed only in the regions where the small pelagic biomass is larger than the 80th percentile (left panel) and 95th percentile (right panel) of all the small pelagic biomass values reported in Fig. S9

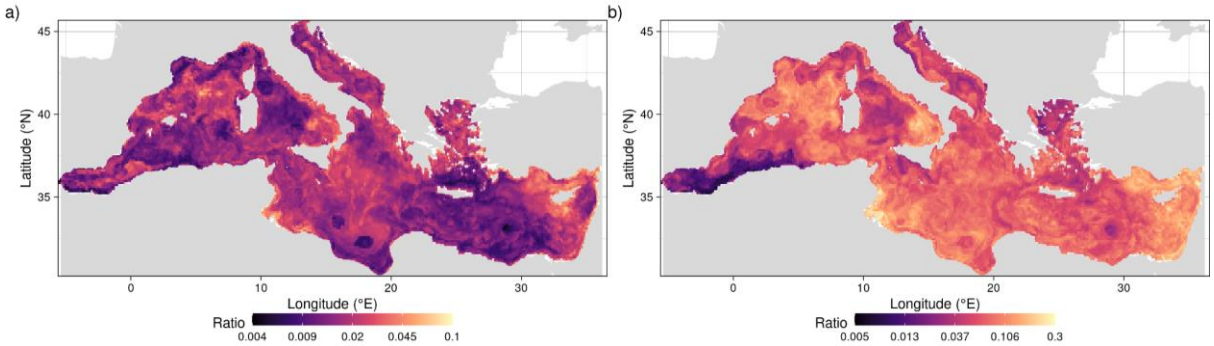

Figure S10: Ratio plastic:plankton for size a) between 0.33 and 1 mm and b) between 1 and 5 mm.

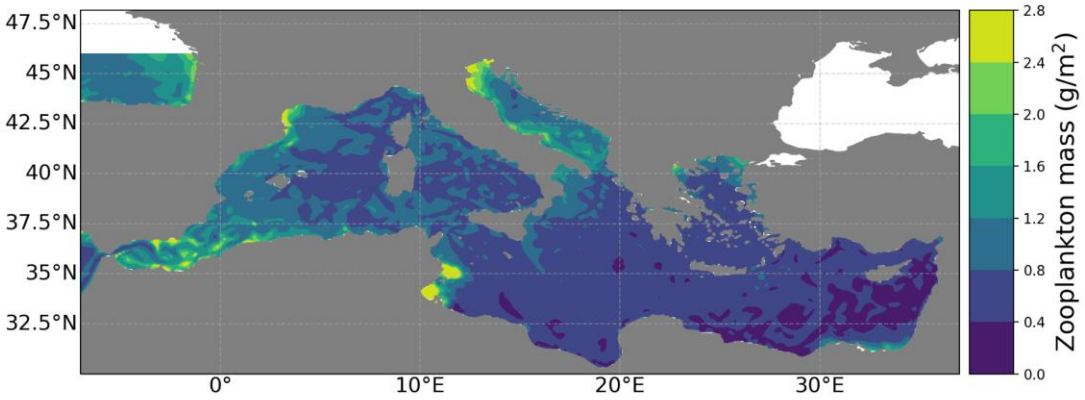

Figure S11: Climatology of zooplankton concentration (expressed as mass content of zooplankton in g/m^2) obtained from GLOBAL_MULTIYEAR_BGC_001_033 product (CMEMS platform) between June and November 2014.